# 2D and 3D shell models for the free vibration investigation of functionally graded cylindrical and spherical panels

# 2D and 3D shell models for the free vibration investigation of functionally graded cylindrical and spherical panels

N. Fantuzzi† , S. Brischetto‡*, F. Tornabene† and E. Viola†

† DICAM Department, University of Bologna

‡ Department of Mechanical and Aerospace Engineering, Politecnico di Torino, Torino, Italy

**Abstract**

*The paper shows the free vibration investigation of simply supported functionally graded material (FGM) shells. Spherical and cylindrical shell geometries are investigated for two different material configurations which are one-layered FGM structures and sandwich structures embedding an internal FGM core. A three-dimensional (3D) exact shell model and different two-dimensional (2D) computational models are compared in terms of frequencies and vibration modes. The proposed numerical solutions are typical 2D finite elements (FEs), and classical and advanced generalized 2D differential quadrature (GDQ) solutions. High and low frequency orders are investigated for thin and thick simply supported shells. Vibration modes are fundamental to compare the 3D exact shell model and 2D numerical solutions. The 2D finite element results based on the classical Reissner-Mindlin theory are calculated using a typical commercial FE software. Classical and advanced GDQ 2D models use the generalized unified formulation. The 3D exact shell model uses the differential equations of equilibrium written in general orthogonal curvilinear coordinates and developed in layer-wise (LW) form. The differences between 2D numerical results and 3D exact results depend on the thickness ratio and geometry of the structure, the considered mode and the frequency order, the lamination sequence and materials.*

**Keywords:** functionally graded materials; cylindrical and spherical shells; finite element solution; exact 3D and numerical 2D shell models; generalized differential quadrature solution; free vibration analysis.

## 1 Introduction

Many engineering structures are subjected to severe thermal and mechanical loads. Typical examples are thermal barrier coatings, rocket nozzles and components for engines. These structures need refractary materials combined with high structural performances. The introduction of Functionally Graded Materials (FGMs) in these structures could be an optimal solution. FGMs usually embed metallic and ceramic phases which vary through the thickness direction with continuity. In this way, the external or internal part could be totally ceramic to conduct the refractory assignment and the opposite part could be totally metallic to carry out the structural assignment [1]. Alternative uses of FGMs were

*Author for Correspondence: Salvatore Brischetto, Department of Mechanical and Aerospace Engineering, Politecnico di Torino, corso Duca degli Abruzzi, 24, 10129 Torino, ITALY. tel: +39.011.090.6813, fax: +39.011.090.6899, e.mail: salvatore.brischetto@polito.it.

discussed in [2] where they were employed to build biological structures where each layer has different specific functions to carry out. These structures are characterized by functional spatially distributed gradients. FGMs have two or more constituent phases that vary their composition through a chosen direction with continuity [3], [4]. They can be considered as a new generation of composite materials with benefits such as a possible decrease of transverse and in-plane stresses through the thickness direction, enhanced thermal properties, a reduced residual stress distribution, higher fracture toughness and lessened stress intensity factors [5], [6]. A further FGM advantage is its use as internal core in the conception of sandwich plates and shells. The FGM core could make possible the continuity of in-plane stresses through the thickness direction. Sandwich structures including conventional and classical cores do not allow this feature [7], [8]. An accurate assessment of strain, displacement and stress components, frequencies and vibration modes is essential in the conception of structural elements embedding FGM layers. For these reasons, classical and new advanced two-dimensional (2D) and three-dimensional (3D) models have been extended to the analysis of plates and shells including FGM layers.

A reliable and accurate numerical approach to solve partial differential systems of equations is the Generalized Differential Quadrature (GDQ) method. The GDQ method is a collocation method and it solves the mathematical problem by means of structured points situated on the structure [9]. 2D GDQ solutions for FGM plate and shell analyses are discussed in [10]- [16]. The 2D static analysis of FGM plates and shells has been proposed in [10] and [11]. The free vibration analysis of shells based on Winkler-Pasternak foundation is described in [12] and [13]. Further general papers about the 2D GDQ method applied to FGMs are described in [14]- [16].

In the literature, 3D models for FGM structures are developed for particular geometries separately and they do not give a general formulation for several geometries (plate, cylindrical panel and spherical panel) as done by Brischetto in [17]- [21]. Dong [22] developed a 3D Chebyshev-Ritz procedure for free vibration analysis of FGM annular plates including several boundary conditions. The Chebyshev-Ritz procedure is also used by Li et al. [23] to investigate free vibrations of FGM rectangular plates. Malekzadeh [24] proposed a semi-analytical differential quadrature model (DQM) based on series solution to solve the motion equations for the free vibration investigation of FGM thick plates based on elastic foundation with two parameters. Hosseini et al. [25] and Vel and Batra [26] developed closed form 3D solutions for the free vibration analysis of functionally graded plates. Other 3D exact models consider the static analysis of FGM plates. The bending of single-layered FGM plates was analyzed in [27] and [28]. The bending of sandwich plates including several FGM cores was proposed in [29]. An exact 3D analysis for a simply supported functionally gradient piezoelectric rectangular plate which was grounded along its four edges was proposed in [30]. Further papers in the literature separately analyze FGM shells. 3D free vibrations of a FGM cylindrical panel embedding piezoelectric layers was proposed by Alibeigloo et al. [31]. In this case, a semi-analytical method and an analytical method for non-simply supported and simply supported boundary conditions were employed, respectively. The free vibrations of FG thick curved shells for different boundary conditions using the 3D elasticity theory combined with the DQM and the trigonometric functions to approximate the governing equations was proposed in [32]. A laminate approximate model was employed by Chen et al. [33] for free vibrations of cylindrically orthotropic FG shells filled with fluid and considering variable thickness values and simply-supported boundary conditions. Vel [34] proposed three-dimensional linear elastodynamics equations simplified to the case of generalized plane strain deformation in the axial direction. Forced and free vibrations of FGM cylindrical shells were analyzed. Sladek et al. [35]- [37] developed a meshless model using the local Petrov-Galerkin method for 3D axisymmetric linear elastic solids having material properties which vary with continuity. The analyzed cases are 3D stress investigation of FGM structures, three-dimensional (3D) heat conduction problem of FGM structures and 3D static and elastodynamic problem for FGM structures.

The present work shows the comparison between the frequencies calculated using the exact 3D shell model, and those calculated using the typical 2D finite element method (FEM) and the classical and

advanced 2D GDQ shell models. The proposed benchmarks are single-layered and sandwich simply supported FGM cylindrical and spherical shells. This paper is a further development of the previous authors' works about the free vibration analysis of multilayered sandwich and composite plates and cylinders [38], multilayered sandwich and composite cylindrical and spherical shells [39], sandwich and single-layered FGM plates and cylinders [40], single- and double-walled carbon nanotubes [41]. The proposed 3D exact shell model was proposed by Brischetto in [17]- [21], where the differential equilibrium equations including general orthogonal curvilinear coordinates were solved in an exact way using the exponential matrix method and harmonic form of displacements in the framework of a layer-wise approach. The 2D FE results were calculated using the commercial finite element code Straus7 [42]. The 2D GDQ shell method has been proposed, by the authors, for several FGM, composite and sandwich structures. First order shear deformation theory (GDQ-FSDT) has been developed for plates, revolution shells and doubly-curved shells in [43]- [48]. A general formulation for advanced two-dimensional models, based on the Carrera's Unified Formulation [49], has been developed for the free vibration analysis of laminated FGM and composite structures in [50] and [51], respectively. Preliminary results for the static analysis of FGM plates were published in [52] and [53] where a stress recovery methodology has been used to calculate the stresses and strains through the thickness of the shell. The same method has been developed for advanced 2D models in [54] and [55] where sandwich composite structures have been analyzed in details.

Exact 3D solutions for the free vibration problem have infinite frequencies because they use infinite degrees of freedom (DOFs). Assumptions in the thickness direction $z$ made for 2D plate and shell models allow the three displacement components in each point to be written in terms of a certain number of DOFs in the thickness direction $z$. 2D numerical models (e.g., the Finite Element (FE) model and the generalized differential quadrature (GDQ) method) have the number of modes equals to a finite number. This number is equal to the total number of used DOFs. Therefore, some modes cannot be obtained using simple models (such as classical numerical two-dimensional methods) [56]. An evaluation of differences between the 2D FE, the 2D GDQ and the 3D exact free frequency results is possible if the vibration mode investigations are performed to see which frequency must be compared. The present work shows a free vibration analysis for single-layered and sandwich FGM cylindrical and spherical shell panels which are simply-supported. Low and high order frequencies and vibration modes are calculated. The fundamental features of higher frequency order analysis have been extensively discussed in the work by Brischetto and Carrera [56], in the works by Leissa [57], [58] and in the monograph by Werner [59].

In the literature, only a few papers investigated higher frequency orders for FGM plates and shells. Works that compare numerical 2D shell models and exact 3D shell models are even less frequent. The present paper aims to examine in depth this feature comparing the free frequencies for FGM cylindrical and spherical shells calculated using the FE commercial code called Straus7, the classical and advanced 2D GDQ shell models, and the 3D exact shell solution. The employed 3D exact method gives results for plates, cylindrical or spherical shell panels, and cylinders. The comparison with the 2D FE code and the 2D GDQ methods is made only for FGM cylindrical and spherical shells because the other geometries, materials and lamination sequences have already been analyzed in past authors' works [38]- [41]. The aim of this work is to explain how to compare the three proposed methods (3D exact, 2D FE and 2D GDQ) and to show the main limits of typical 2D models for the FGM cylindrical and spherical panel free vibration analysis.

## 2 Exact 3D shell model

The strain-displacement relations in orthogonal curvilinear coordinates $(\alpha, \beta, z)$ for the three-dimensional theory of elasticity are written in this work for a generic $k^{th}$ layer of the multilayered shell including FGM layers having constant radii of curvature (details can be found in Figure 1), further information

are given in [57], [58] and [60]:

$$\epsilon^k_{\alpha\alpha} = \frac{1}{H_\alpha}\frac{\partial u^k}{\partial \alpha} + \frac{w^k}{H_\alpha R_\alpha} \,, \tag{1}$$

$$\epsilon^k_{\beta\beta} = \frac{1}{H_\beta}\frac{\partial v^k}{\partial \beta} + \frac{w^k}{H_\beta R_\beta} \,, \tag{2}$$

$$\epsilon^k_{zz} = \frac{\partial w^k}{\partial z} \,, \tag{3}$$

$$\gamma^k_{\beta z} = \frac{1}{H_\beta}\frac{\partial w^k}{\partial \beta} + \frac{\partial v^k}{\partial z} - \frac{v^k}{H_\beta R_\beta} \,, \tag{4}$$

$$\gamma^k_{\alpha z} = \frac{1}{H_\alpha}\frac{\partial w^k}{\partial \alpha} + \frac{\partial u^k}{\partial z} - \frac{u^k}{H_\alpha R_\alpha} \,, \tag{5}$$

$$\gamma^k_{\alpha\beta} = \frac{1}{H_\alpha}\frac{\partial v^k}{\partial \alpha} + \frac{1}{H_\beta}\frac{\partial u^k}{\partial \beta} \,. \tag{6}$$

The parametric coefficients in the case of shells having constant radii of curvature can be written as:

$$H_\alpha = \left(1 + \frac{z}{R_\alpha}\right) = \left(1 + \frac{\tilde{z} - h/2}{R_\alpha}\right) \,, \quad H_\beta = \left(1 + \frac{z}{R_\beta}\right) = \left(1 + \frac{\tilde{z} - h/2}{R_\beta}\right) \,, \quad H_z = 1 \,, \tag{7}$$

where $h$ is the global thickness of the shell. $H_\alpha$ and $H_\beta$ depend on $z$ or $\tilde{z}$ coordinate (see Figure 2). $H_z = 1$ because $z$ coordinate is not curvilinear. $R_\alpha$ and $R_\beta$ are the principal radii of curvature in the $\alpha$ and $\beta$ directions, respectively. Operator $\partial$ is used to indicate the partial derivatives. Geometrical equations for spherical shells in Eqs.(1)-(6) include geometrical equations for cylindrical shells when $R_\alpha$ or $R_\beta$ is infinite (with $H_\alpha$ or $H_\beta$ equals one). They include geometrical relations for plates when both $R_\alpha$ and $R_\beta$ are infinite (with $H_\alpha = H_\beta = 1$) (further details can be found in [57], [58] and [60]).

The three differential equilibrium equations, developed for the free frequency problem of multilayered spherical shells having radii of curvature $R_\alpha$ and $R_\beta$ which are constant, are here proposed (the most general form is given in [61] and [62] for variable radii of curvature):

$$H_\beta\frac{\partial \sigma^k_{\alpha\alpha}}{\partial \alpha} + H_\alpha\frac{\partial \sigma^k_{\alpha\beta}}{\partial \beta} + H_\alpha H_\beta\frac{\partial \sigma^k_{\alpha z}}{\partial z} + \left(\frac{2H_\beta}{R_\alpha} + \frac{H_\alpha}{R_\beta}\right)\sigma^k_{\alpha z} = \rho^k(z) H_\alpha H_\beta \ddot{u}^k \,, \tag{8}$$

$$H_\beta\frac{\partial \sigma^k_{\alpha\beta}}{\partial \alpha} + H_\alpha\frac{\partial \sigma^k_{\beta\beta}}{\partial \beta} + H_\alpha H_\beta\frac{\partial \sigma^k_{\beta z}}{\partial z} + \left(\frac{2H_\alpha}{R_\beta} + \frac{H_\beta}{R_\alpha}\right)\sigma^k_{\beta z} = \rho^k(z) H_\alpha H_\beta \ddot{v}^k \,, \tag{9}$$

$$H_\beta\frac{\partial \sigma^k_{\alpha z}}{\partial \alpha} + H_\alpha\frac{\partial \sigma^k_{\beta z}}{\partial \beta} + H_\alpha H_\beta\frac{\partial \sigma^k_{zz}}{\partial z} - \frac{H_\beta}{R_\alpha}\sigma^k_{\alpha\alpha} - \frac{H_\alpha}{R_\beta}\sigma^k_{\beta\beta} + \left(\frac{H_\beta}{R_\alpha} + \frac{H_\alpha}{R_\beta}\right)\sigma^k_{zz} = \rho^k(z) H_\alpha H_\beta \ddot{w}^k \,, \tag{10}$$

where $\rho^k(z)$ is the mass density varying through the $z$ direction of an FGM layer. $(\sigma^k_{\alpha\alpha}, \sigma^k_{\beta\beta}, \sigma^k_{zz}, \sigma^k_{\beta z}, \sigma^k_{\alpha z}, \sigma^k_{\alpha\beta})$ are the six stress components. $\ddot{u}^k$, $\ddot{v}^k$ and $\ddot{w}^k$ are the second temporal derivative of the three displacement components $u^k$, $v^k$ and $w^k$, respectively. Each variable depends on the $k^{th}$ layer. $R_\alpha$ and $R_\beta$ are considered at the mid-surface $\Omega_0$ of the whole multilayered shell. $H_\alpha$ and $H_\beta$ vary through the $z$ direction of the multilayered shell with continuity. These equilibrium equations, written for spherical shell panels, degenerate into equilibrium equations for cylindrical shell panels and cylinders when $R_\alpha$ or $R_\beta$ is infinite ($H_\alpha$ or $H_\beta$ equals 1), and in equilibrium equations for plate geometries when both $R_\alpha$ and $R_\beta$ are infinite ($H_\alpha = H_\beta = 1$).

The closed form of Eqs.(8)-(10) is obtained for simply supported shells. In these cases, the three

displacement components have the following harmonic form:

$$u^k(\alpha,\beta,z,t) = U^k(z)e^{i\omega t}cos(\bar{\alpha}\alpha)sin(\bar{\beta}\beta)\ , \tag{11}$$

$$v^k(\alpha,\beta,z,t) = V^k(z)e^{i\omega t}sin(\bar{\alpha}\alpha)cos(\bar{\beta}\beta)\ , \tag{12}$$

$$w^k(\alpha,\beta,z,t) = W^k(z)e^{i\omega t}sin(\bar{\alpha}\alpha)sin(\bar{\beta}\beta)\ , \tag{13}$$

where $U^k(z)$, $V^k(z)$ and $W^k(z)$ are the displacement amplitudes in $\alpha$, $\beta$ and $z$ directions, respectively. $i$ is the coefficient of the imaginary unit. $\omega = 2\pi f$ is the circular frequency where $f$ is the frequency value, $t$ is the time. In coefficients $\bar{\alpha} = \frac{m\pi}{a}$ and $\bar{\beta} = \frac{n\pi}{b}$, $m$ and $n$ are the half-wave numbers and $a$ and $b$ are the shell dimensions in $\alpha$ and $\beta$ directions, respectively (calculated in the mid-surface $\Omega_0$).

Three-dimensional linear elastic constitutive equations in orthogonal curvilinear coordinates ($\alpha$, $\beta$, $z$) (see the reference system in Figure 1) are proposed in this section for a generic isotropic $k$ layer. Coefficients $C_{qr}$ depend on the thickness coordinate $z$ for a functionally graded material. The stress components ($\sigma_{\alpha\alpha}$, $\sigma_{\beta\beta}$, $\sigma_{zz}$, $\sigma_{\beta z}$, $\sigma_{\alpha z}$, $\sigma_{\alpha\beta}$) and the strain components ($\epsilon_{\alpha\alpha}$, $\epsilon_{\beta\beta}$, $\epsilon_{zz}$, $\gamma_{\beta z}$, $\gamma_{\alpha z}$, $\gamma_{\alpha\beta}$) are linked, for each $k$ FGM layer, by:

$$\sigma^k_{\alpha\alpha} = C^k_{11}(z)\epsilon^k_{\alpha\alpha} + C^k_{12}(z)\epsilon^k_{\beta\beta} + C^k_{13}(z)\epsilon^k_{zz}\ , \tag{14}$$

$$\sigma^k_{\beta\beta} = C^k_{12}(z)\epsilon^k_{\alpha\alpha} + C^k_{22}(z)\epsilon^k_{\beta\beta} + C^k_{23}(z)\epsilon^k_{zz}\ , \tag{15}$$

$$\sigma^k_{zz} = C^k_{13}(z)\epsilon^k_{\alpha\alpha} + C^k_{23}(z)\epsilon^k_{\beta\beta} + C^k_{33}(z)\epsilon^k_{zz}\ , \tag{16}$$

$$\sigma^k_{\beta z} = C^k_{44}(z)\gamma^k_{\beta z}\ , \tag{17}$$

$$\sigma^k_{\alpha z} = C^k_{55}(z)\gamma^k_{\alpha z}\ , \tag{18}$$

$$\sigma^k_{\alpha\beta} = C^k_{66}(z)\gamma^k_{\alpha\beta}\ . \tag{19}$$

Eqs.(1)-(6), (11)-(13) and (14)-(19) are substituted in Eqs.(8)-(10) to write the system of equations for the $j^{th}$ mathematical layer:

$$\begin{aligned}
&\Big(-\frac{C^j_{55}H_\beta}{H_\alpha R^2_\alpha} - \frac{C^j_{55}}{R_\alpha R_\beta} - \bar{\alpha}^2\frac{C^j_{11}H_\beta}{H_\alpha} - \bar{\beta}^2\frac{C^j_{66}H_\alpha}{H_\beta} + \rho^j H_\alpha H_\beta\omega^2\Big)U^j + \Big(-\bar{\alpha}\bar{\beta}C^j_{12} - \bar{\alpha}\bar{\beta}C^j_{66}\Big)V^j + \\
&\Big(\bar{\alpha}\frac{C^j_{11}H_\beta}{H_\alpha R_\alpha} + \bar{\alpha}\frac{C^j_{12}}{R_\beta} + \bar{\alpha}\frac{C^j_{55}H_\beta}{H_\alpha R_\alpha} + \bar{\alpha}\frac{C^j_{55}}{R_\beta}\Big)W^j + \Big(\frac{C^j_{55}H_\beta}{R_\alpha} + \frac{C^j_{55}H_\alpha}{R_\beta}\Big)U^j_{,z} + \Big(\bar{\alpha}C^j_{13}H_\beta + \\
&\bar{\alpha}C^j_{55}H_\beta\Big)W^j_{,z} + \Big(C^j_{55}H_\alpha H_\beta\Big)U^j_{,zz} = 0\ ,
\end{aligned} \tag{20}$$

$$\begin{aligned}
&\Big(-\bar{\alpha}\bar{\beta}C^j_{66} - \bar{\alpha}\bar{\beta}C^j_{12}\Big)U^j + \Big(-\frac{C^j_{44}H_\alpha}{H_\beta R^2_\beta} - \frac{C^j_{44}}{R_\alpha R_\beta} - \bar{\alpha}^2\frac{C^j_{66}H_\beta}{H_\alpha} - \bar{\beta}^2\frac{C^j_{22}H_\alpha}{H_\beta} + \rho^j H_\alpha H_\beta\omega^2\Big)V^j + \\
&\Big(\bar{\beta}\frac{C^j_{44}H_\alpha}{H_\beta R_\beta} + \bar{\beta}\frac{C^j_{44}}{R_\alpha} + \bar{\beta}\frac{C^j_{22}H_\alpha}{H_\beta R_\beta} + \bar{\beta}\frac{C^j_{12}}{R_\alpha}\Big)W^j + \Big(\frac{C^j_{44}H_\alpha}{R_\beta} + \frac{C^j_{44}H_\beta}{R_\alpha}\Big)V^j_{,z} + \Big(\bar{\beta}C^j_{44}H_\alpha + \\
&\bar{\beta}C^j_{23}H_\alpha\Big)W^j_{,z} + \Big(C^j_{44}H_\alpha H_\beta\Big)V^j_{,zz} = 0\ ,
\end{aligned} \tag{21}$$

$$\begin{aligned}
&\Big(\bar{\alpha}\frac{C^j_{55}H_\beta}{H_\alpha R_\alpha} - \bar{\alpha}\frac{C^j_{13}}{R_\beta} + \bar{\alpha}\frac{C^j_{11}H_\beta}{H_\alpha R_\alpha} + \bar{\alpha}\frac{C^j_{12}}{R_\beta}\Big)U^j + \Big(\bar{\beta}\frac{C^j_{44}H_\alpha}{H_\beta R_\beta} - \bar{\beta}\frac{C^j_{23}}{R_\alpha} + \bar{\beta}\frac{C^j_{22}H_\alpha}{H_\beta R_\beta} + \bar{\beta}\frac{C^j_{12}}{R_\alpha}\Big)V^j + \\
&\Big(\frac{C^j_{13}}{R_\alpha R_\beta} + \frac{C^j_{23}}{R_\alpha R_\beta} - \frac{C^j_{11}H_\beta}{H_\alpha R^2_\alpha} - \frac{2C^j_{12}}{R_\alpha R_\beta} - \frac{C^j_{22}H_\alpha}{H_\beta R^2_\beta} - \bar{\alpha}^2\frac{C^j_{55}H_\beta}{H_\alpha} - \bar{\beta}^2\frac{C^j_{44}H_\alpha}{H_\beta} + \rho^j H_\alpha H_\beta\omega^2\Big)W^j + \\
&\Big(-\bar{\alpha}C^j_{55}H_\beta - \bar{\alpha}C^j_{13}H_\beta\Big)U^j_{,z} + \Big(-\bar{\beta}C^j_{44}H_\alpha - \bar{\beta}C^j_{23}H_\alpha\Big)V^j_{,z} + \Big(\frac{C^j_{33}H_\beta}{R_\alpha} + \frac{C^j_{33}H_\alpha}{R_\beta}\Big)W^j_{,z} + \\
&\Big(C^j_{33}H_\alpha H_\beta\Big)W^j_{,zz} = 0\,.
\end{aligned} \tag{22}$$

Elastic coefficients $C_{qr}$ in the case of FGM layers depend on the thickness coordinate $z$. Parametric coefficients $H_\alpha$ and $H_\beta$ are variables depending on the thickness coordinate $z$. Therefore, equilibrium equations have coefficients depending on the $z$ coordinate. Eqs.(20)-(22) with constant coefficients are possible when each $k$ layer is splitted in $l$ mathematical layers where the coefficients $C_{qr}$ are calculated as constant and geometrical coefficients $H_\alpha$ and $H_\beta$ are easily evaluated in the middle of each mathematical layer. Eqs.(20)-(22) have been rewritten using $j = k \times l$ mathematical layers in order to obtain constant coefficients (see [17] for further information).

Mass density and elastic coefficients are considered as constant in the $j^{th}$ mathematical layer even when a functionally graded material is included in the structure. Parametric coefficients $H_\alpha$ and $H_\beta$ are also constant when they are calculated with the thickness coordinate $z$ considered in the middle of the $j^{th}$ layer. The system of Eqs.(20)-(22) can be developed in a compact form. The symbol $A_s^j$ (where $s$ varies from 1 to 19 and $j$ from 1 to the $N_L$ mathematical layer) is used for terms defined by parentheses which multiply the displacements and their derivatives with respect the $z$ coordinate:

$$A_1^j U^j + A_2^j V^j + A_3^j W^j + A_4^j U_{,z}^j + A_5^j W_{,z}^j + A_6^j U_{,zz}^j = 0 \ , \tag{23}$$

$$A_7^j U^j + A_8^j V^j + A_9^j W^j + A_{10}^j V_{,z}^j + A_{11}^j W_{,z}^j + A_{12}^j V_{,zz}^j = 0 \ , \tag{24}$$

$$A_{13}^j U^j + A_{14}^j V^j + A_{15}^j W^j + A_{16}^j U_{,z}^j + A_{17}^j V_{,z}^j + A_{18}^j W_{,z}^j + A_{19}^j W_{,zz}^j = 0 \ . \tag{25}$$

Eqs.(23)-(25) are a system of three second order differential equations. They were developed for spherical shell panels having constant radii of curvature and they include relations for cylindrical shell panels and plates.

The system of second order differential equations is transformed into a system of first order differential equations in analogy with the methodology seen in [63] and [64]. The compact form for the first order differential equation system is:

$$\boldsymbol{D}^j \frac{\partial \boldsymbol{U}^j}{\partial \tilde{z}} = \boldsymbol{A}^j \boldsymbol{U}^j \ , \tag{26}$$

where $\frac{\partial \boldsymbol{U}^j}{\partial \tilde{z}} = \boldsymbol{U}^{j\prime}$ and $\boldsymbol{U}^j = [U^j \ V^j \ W^j \ U^{j\prime} \ V^{j\prime} \ W^{j\prime}]$. Eq.(26) can be given as:

$$\boldsymbol{D}^j \boldsymbol{U}^{j\prime} = \boldsymbol{A}^j \boldsymbol{U}^j \ , \tag{27}$$

$$\boldsymbol{U}^{j\prime} = \boldsymbol{D}^{j-1} \boldsymbol{A}^j \ \boldsymbol{U}^j \ , \tag{28}$$

$$\boldsymbol{U}^{j\prime} = \boldsymbol{A}^{j*} \ \boldsymbol{U}^j \ , \tag{29}$$

with $\boldsymbol{A}^{j*} = \boldsymbol{D}^{j-1} \boldsymbol{A}^j$.

The solution of Eq.(29) can be developed as (see [64] and [65]):

$$\boldsymbol{U}^j(\tilde{z}^j) = exp(\boldsymbol{A}^{j*} \tilde{z}^j) \boldsymbol{U}^j(0) \quad \text{with} \quad \tilde{z}^j \ \epsilon \ [0, h^j] \ , \tag{30}$$

where $\tilde{z}^j$ is the thickness coordinate for the $j^{th}$ layer from 0 at the bottom to $h^j$ at the top (see Figure 2). The exponential matrix is expanded with $\tilde{z}^j = h^j$ for each $j$ layer:

$$\boldsymbol{A}^{j**} = exp(\boldsymbol{A}^{j*} h^j) = \boldsymbol{I} + \boldsymbol{A}^{j*} h^j + \frac{\boldsymbol{A}^{j*2}}{2!} h^{j2} + \frac{\boldsymbol{A}^{j*3}}{3!} h^{j3} + \ldots + \frac{\boldsymbol{A}^{j*N}}{N!} h^{jN} \ , \tag{31}$$

$\boldsymbol{I}$ is the identity matrix with dimension $6 \times 6$. The convergence of this expansion is very fast as demonstrated in [66] and it is not time consuming from the computational point of view. The proposed methodology has already been applied in [67] for the plate cases using rectilinear orthogonal coordinates ($x$,$y$,$z$) and in [68] for the cylinders using cylindrical coordinates ($\rho$,$\theta$).

Considering $j = N_L$ layers, $N_L - 1$ transfer matrices must be calculated using for each interface the interlaminar continuity conditions of displacements and transverse shear/normal stresses. Moreover,

the structures must be considered as simply supported and free stresses at the top and at the bottom. The described conditions allow the final system to be obtained from that in Eqs. (23)-(25):

$$\boldsymbol{E}\,\boldsymbol{U}^1(0) \;=\; \mathbf{0}\,, \tag{32}$$

matrix $\boldsymbol{E}$ presents $(6 \times 6)$ dimension independently from the number of layers $N_L$, even if a layer-wise method is employed. $\boldsymbol{U}^1(0)$ is $\boldsymbol{U}$ evaluated at the bottom of the multilayered shell (first layer 1 with $\tilde{z}^1 = 0$). Further information about this method, and all the mathematical steps missed in the present paper have been given in [17], [18] and [19] where this 3D exact shell method has been developed and described in details.

The free vibration analysis consists to calculate the non-trivial solution of $\boldsymbol{U}^1(0)$ in Eq.(32) considering the determinant of matrix $\boldsymbol{E}$ equals zero:

$$det[\boldsymbol{E}] = 0\,, \tag{33}$$

Eq.(33) allows the roots of an higher order polynomial in $\lambda = \omega^2$ to be found. For each imposed half-wave number $(m, n)$ couples, a certain number of circular frequencies (from I to $\infty$) are calculated. This value depends on the order $N$ used for the $j^{th}$ exponential matrix $\boldsymbol{A}^{j\,**}$ and the number $N_L$ of mathematical layers.

A certain number of circular frequencies $\omega_s$ are calculated when half-wave number $(m, n)$ couples are imposed in the plates and shells. For each circular frequency $\omega_s$, the vibration mode through the thickness direction in terms of the three displacement components $u$, $v$ and $w$ is evaluated.

## 3 Refined 2D GDQ shell models

This study considers two refined and one classical 2D shell models for the numerical benchmarks that will be analyzed in Section 5. These theories are placed within the framework of an equivalent single layer approach based on the Carrera's Unified Formulation [49]. The displacement field is presented in generalized form as described in [51]:

$$\mathbf{U} = \sum_{\tau=0}^{N_c+1} \mathbf{F}_\tau \mathbf{u}^{(\tau)}\,, \tag{34}$$

where $\mathbf{U}$ are the 3D displacement components and $\mathbf{u}$ indicates the vector of the $\tau^{th}$ generalized displacements of the points on the middle surface of the structure [51]. $\mathbf{F}_{\tau(ij)} = \delta_{ij} F_\tau$, for $i, j = 1, 2, 3$ is the matrix for the thickness functions and $\delta$ is the Kronecker delta function. Using the general higher-order method, the classical first order model can be obtained when $\tau = 0, 1$ or $N_c = 0$ (GDQ-FSDT), which corresponds to the classic linear theory developed by Reissner and Mindlin. A higher-order expansion with $N_c = 4$ and the inclusion of the Murakami zigzag function is called GDQ-ZZ. Since considering the ZZ function for single layered structures is trivial, it is added only for multilayered shells. Hence, the same model without the ZZ function is termed GDQ-HOST.

The main advantage of this approach is that it is possible to change the order of the theory $\tau$ without changing the whole implementation. From the mechanics, the relation between generalized strains $\boldsymbol{\varepsilon}^{(\tau)}$ and displacement parameters $\mathbf{u}^{(\tau)}$ is obtained, according to [51], as:

$$\boldsymbol{\varepsilon}^{(\tau)} = \mathbf{D}_\Omega \mathbf{u}^{(\tau)} \quad \text{for} \quad \tau = 0, 1, 2, \ldots, N_c, N_c + 1\,, \tag{35}$$

where $\mathbf{D}_\Omega$ was fully described in [51].

The $\tau^{th}$ order resultants using generalized $s^{th}$ order strains $\boldsymbol{\varepsilon}^{(s)}$ is written as:

$$\mathbf{S}^{(\tau)} = \sum_{s=0}^{N_c+1} \mathbf{A}^{(\tau s)} \boldsymbol{\varepsilon}^{(s)} \quad \text{for} \quad \tau = 0, 1, 2, \ldots, N_c, N_c + 1\,, \tag{36}$$

the elastic coefficients for the matrix $\mathbf{A}^{(\tau s)} = \sum_{k=1}^{N_L} \int_{z_k}^{z_{k+1}} \left(\mathbf{Z}^{(\tau)}\right)^T \bar{\mathbf{C}}^{(k)} \mathbf{Z}^{(s)} H_\alpha H_\beta dz$ are reported and deeply commented in [51]. $\bar{\mathbf{C}}^{(k)}$ is the constitutive matrix for the $k^{th}$ ply and $\mathbf{Z}^{(\tau)}$ is the matrix for geometrical terms.

The result of this mathematical framework is a three motion equation core that is function of the internal actions as:

$$\mathbf{D}_\Omega^\star \mathbf{S}^{(\tau)} = \sum_{s=0}^{N_c+1} \mathbf{M}^{(\tau s)} \ddot{\mathbf{u}}^{(s)} \quad \text{for} \quad \tau = 0, 1, 2, \ldots, N_c, N_c + 1 \,, \tag{37}$$

where $\mathbf{D}_\Omega^\star$ is the equilibrium operator and $\mathbf{M}^{(\tau s)}$ is the inertial matrix [51]. In detail, the inertial matrix $\mathbf{M}_{(ij)}^{(\tau s)} = \delta_{ij} I_0^{(\tau s)}$ contains the inertial mass terms $I_0^{(\tau s)}$ for $i, j = 1, 2, 3$ and they can be evaluated as:

$$I_0^{(\tau s)} = \sum_{k=1}^{N_L} \int_{z_k}^{z_{k+1}} \rho^{(k)} F_\tau F_s H_\alpha H_\beta dz \quad \text{for} \quad \tau, s = 0, 1, 2, \ldots, N_c, N_c + 1 \,, \tag{38}$$

where $\rho^{(k)}$ is the mass density of the material per unit of volume of the $k^{th}$ ply. The combination of the Eqs. (35), (36) and (37) gives the equilibrium equations as a function of the displacement parameters:

$$\sum_{s=0}^{N_c+1} \mathbf{L}^{(\tau s)} \mathbf{u}^{(s)} = \sum_{s=0}^{N_c+1} \mathbf{M}^{(\tau s)} \ddot{\mathbf{u}}^{(s)} \quad \text{for} \quad \tau = 0, 1, 2, \ldots, N_c, N_c + 1 \,, \tag{39}$$

where $\mathbf{L}^{(\tau s)} = \mathbf{D}_\Omega^\star \mathbf{A}^{(\tau s)} \mathbf{D}_\Omega$ is the fundamental operator. This operation is described in detail in [51].

Boundary conditions are included for the solution of the differential problem of Eq. (39). Combining conveniently the static and kinematic conditions, any type of boundary conditions is considered. The main advantage of using a numerical approach, such as the GDQ method, is that any boundary condition can be implemented, as already demonstrated in [51]. However, the main aim of the present paper is to present the accuracy of GDQ method when compared to an exact 3D analysis which can study only simply-supported boundary conditions:

$$\begin{aligned} N_\alpha^{(\tau)} = 0,\ u_\beta^{(\tau)} = u_z^{(\tau)} = 0 \quad \tau = 0, 1, 2, \ldots, N_c, N_c + 1 \quad \text{at} \quad \alpha = \alpha^0 \quad \text{or} \quad \alpha = \alpha^1 \quad \beta^0 \leq \beta \leq \beta^1 \,, \\ u_\alpha^{(\tau)} = 0,\ N_\beta^{(\tau)} = 0,\ u_z^{(\tau)} = 0 \quad \tau = 0, 1, 2, \ldots, N_c, N_c + 1 \quad \text{at} \quad \beta = \beta^0 \quad \text{or} \quad \beta = \beta^1 \quad \alpha^0 \leq \alpha \leq \alpha^1 \,. \end{aligned} \tag{40}$$

# 4 Two-dimensional finite element model

The two-dimensional (2D) finite element results analyzed in this work have been calculated using the FE commercial code Straus7 [42]. Straus7 is a fully-integrated visual environment combined with a suite of powerful solvers. This FE code implements different types of elements. 4-node 2D elements (QUAD4) have been considered for the present applications. The displacement model employed by Straus7 in these 2D FEs is based on the Reissner-Mindlin hypotheses (constant transverse displacement through the thickness direction $z$ and equivalent single layer approach that mean zero transverse normal strain). Straus7 does not include any devoted tool for the FGM structural analyses. For these reasons, each FGM layer has been splitted into a number $N_L$ of $j$ mathematical layers with constant mass density and Young modulus. They are equal to the mean value of each $j^{th}$ layer. Straus7 has been tested and validated considering the FGM plates and shells as multilayered structures embedding $N_L$ mathematical layers with constant properties. The previous published benchmarks regarding 2D FEs [69]- [73] demonstrated that GDQ and FE methods give very close results, in particular for the vibration problems. QUAD4 is a good choice for this type of analysis, even if other types of element can be used. A review of the

validations and comparisons between the Straus7 FE models and the GDQ method can be found in the books [74] and [61].

# 5 Results

This part shows an extensive comparison between the 2D FE model, classical and advanced two-dimensional (2D) GDQ models and the exact three-dimensional (3D) shell solution described in the previous sections. The comparisons are proposed for cylindrical and spherical shells and several laminations and materials. Before this comparison, the three different methods will be validated in opportune sections in order to use them with confidence in the new benchmarks proposed.

## 5.1 Preliminary assessments

Preliminary assessments are proposed to validate the three different methods and in particular to understand the mesh and the shell element to use in the Finite Element results via Straus7, the Chebyshev-Gauss-Lobatto grid to use for 2D GDQ results and the order for the exponential matrix and the number of fictitious layers to use in the 3D exact results.

### 5.1.1 Validation of the two-dimensional (2D) FE method

In the validation and convergence study of the 2D FE method, the same geometries and materials used for the validation of 2D GDQ models in Section 5.1.2 and for the new benchmarks in Section 5.2 will be considered. Such cases will be presented in details in this section and it will be also used in the next sections. A cylindrical and a spherical shell panel will be considered as shown in Figure 3. The cylindrical shell has a radius of curvature $R_\alpha = 10m$ and an infinite radius of curvature $R_\beta$ in $\beta$ direction. The dimensions are $a = \frac{\pi}{3}R_\alpha$ and $b = 20m$, and the thickness ratios are $R_\alpha/h = 1000$, 100, 10, 5. The spherical shell has radii of curvature $R_\alpha = R_\beta = 10m$, dimensions $a = b = \frac{\pi}{3}R_\alpha$, and thickness ratios $R_\alpha/h = 1000$, 100, 10, 5.

The two structures will be analyzed as isotropic single-layered FGM ($h_1 = h$) and as a sandwich embedding an FGM core and two external skins (skins with $h_1 = h_3 = 0.15h$ and core with $h_2 = 0.7h$). Figure 4 shows the two proposed material configurations.

The single-layered FGM configuration shows the Young modulus and the mass density as indicated in the following equations:

$$E(z) = E_m + (E_c - E_m)V_c\,, \tag{41}$$

$$\rho(z) = \rho_m + (\rho_c - \rho_m)V_c\,, \tag{42}$$

where $V_c$ is the volume fraction for the ceramic phase, it varies through the $z$ direction with continuity:

$$V_c = (0.5 + z/h)^p\,, \tag{43}$$

$z$ varies from $-h_1/2$ to $h_1/2$. The bottom is completely metallic (m) (Aluminium Alloy Al2024: Young modulus $E_m = 73GPa$, mass density $\rho_m = 2800kg/m^3$ and Poisson ratio $\nu_m = 0.3$) and the top is completely ceramic (c) (Alumina $Al_2O_3$: Young modulus $E_c = 380GPa$, mass density $\rho_c = 3800kg/m^3$ and Poisson ratio $\nu_c = 0.3$). The Poisson ratio is assumed as constant through the $z$ direction. Mass density and Young modulus are variable through the thickness direction using the laws shown in Eqs.(41)-(42) where the volume fraction of the ceramic phase is indicated in Eq.(43) ($V_c = 0$ at the bottom and $V_c = 1$ at the top). The exponents $p$ of the FGM law are $p$ equal 0.0, 0.5, 1.0, 2.0. $p = 0.0$ is used for completely ceramic structures.

The second configuration considers a sandwich as shown in Figure 4. The skin at the bottom is metallic (the same Aluminum Alloy Al2024 used in the first configuration) and the skin at the top is

a ceramic with different properties from those of the Alumina $Al_2O_3$ used for the first configuration (Young modulus $E_c = 200GPa$, mass density $\rho_c = 5700kg/m^3$ and Poisson ratio $\nu_c = 0.3$). The FGM core has constant Poisson ratio. Mass density and Young modulus show the same through-the-thickness variation already indicated for the first single-layered FGM case in Eqs.(41) and (42). The $p$ exponents are 0.5, 1.0 and 2.0. A classical core can also be included when material properties are calculated as the mean value between the values at the top skin and those at the bottom skin ($E = \frac{E_c+E_m}{2}$, $\rho = \frac{\rho_c+\rho_m}{2}$ and Poisson ratio $\nu = 0.3$). The thickness value substituted in Eq.(43) is $h_c = 0.7h$ in the case of FGM core.

For this convergence and validation study, 4-node 2D elements (QUAD4) have been considered. Two cases are proposed: a single-layered FGM cylindrical shell panel having $p$=0.0 and a sandwich spherical shell panel embedding an FGM core with $p$=1.0. For both cases, two different thickness ratios have been investigated: thick shells with $R_\alpha/h = 10$ and thin shells with $R_\alpha/h = 100$. The Straus7 code does not include any specific tool for FGM plates and shells, for this reason the FGM law through the thickness direction has been described by means of 100 mathematical layers having constant properties. In the past authors' work [40] and in the next validation of the 3D exact shell model, it has been demonstrated as 100 mathematical layers are sufficient to correctly describe any FGM law. Results for the cylindrical shell and for the spherical shell are shown in Tables 1 and 2, respectively. From Tables 1 and 2 it can be deducted that a $100 \times 100$ mesh is sufficient for a correct analysis. In all the results proposed in Section 5.2, the 2D FE analyses have been performed with the 4-node 2D element (QUAD4) of Straus7 using 100 mathematical layers for the FGM description and a $100 \times 100$ mesh.

### 5.1.2 Validation of 2D GDQ models

The accuracy and stability of the GDQ models have been demonstrated in different works given in the literature [43]- [55]. In general, the GDQ method uses a very reduced number of points to find an accurate and valid solution. For plates, the solution is accurate for a number of points smaller than shell cases [43]- [55]. These features are demonstrated by the following convergence analyses. A cylindrical and a spherical panel are considered. Both geometries have already been described in details in Section 5.1.1. Two thickness ratios are used that are $R_\alpha/h$=5 and $R_\alpha/h$=100 with a sandwich scheme considering $h_1 = h_3 = 0.15h$ and $h_2 = 0.7h$. The bottom lamina is made of Aluminum (the same properties seen in the sandwich case of Section 5.1.1). The top lamina is made of Alumina (the same properties seen in the sandwich case of Section 5.1.1). The core has a FGM distribution with $p$=1.0 (see Eqs.(41)-(43) and Figure 4). All the geometries reach a stable trend for $I_N = I_M = 11$, but for all the computations a grid of $I_N = I_M = 25$ is set. The points are located as a Chebyshev-Gauss-Lobatto grid [39], the points used in the $\alpha$ and $\beta$ directions are not-uniformly distributed and they use a cosine function. Figures 5 and 6 show the converge trends for a cylindrical panel (with $h$=2$m$ and $h$=0.1$m$) and for a spherical panel (with $h$=2$m$ and $h$=0.1$m$), respectively, using the error in percentage versus the number of grid points.

### 5.1.3 3D exact model validation

The 3D exact shell model has been tested using a comparison with the three-dimensional differential quadrature model proposed in Zahedinejad et al. [32]. This assessment proposes a simply supported cylindrical shell panel with the two coincident dimensions $a$=$b$, the investigated thickness ratio is $a/h = 5$. Two different radii of curvature $R_\alpha$ are used, which allow $a/R_\alpha$ equals 0.5 or 1. The radius of curvature $R_\beta$ in $\beta$ direction is infinite. The shell is single-layered including a functionally graded material as proposed in the left side of Figure 4. The shell is completely metallic at the bottom and completely ceramic at the top. The volume fraction for the ceramic phase $V_c$ has already been described in Eq.(43). The Young modulus and the mass density have the through-the-thickness distribution already seen in Eqs.(41) and (42). The metallic (m) material has Young modulus $E_m = 70GPa$, mass

density $\rho_m = 2702kg/m^3$ and Poisson ratio $\nu_m = 0.3$. The ceramic (c) material considers Young modulus $E_c = 380GPa$, mass density $\rho_c = 3800kg/m^3$ and Poisson ratio $\nu_c = 0.3$. These material data can also be found in [32], where a three-dimensional differential quadrature method is proposed in the case of the free vibration investigation for the cylindrical shell panel when half-wave numbers $m = n = 1$ are imposed and different values for the exponent $p$ are used. The results are shown as dimensionless circular frequencies $\bar{\omega} = \omega h\sqrt{\frac{\rho_c}{E_c}}$. Table 3 confirms that the proposed 3D exact shell model provides results similar to those calculated with the model developed in [32]. The small differences are explained by the fact that the present 3D shell model is exactly solved while the 3D model in [32] is solved using the differential quadrature method which is a numerical solution.

In the present assessment, the proposed 3D solution uses $N_L = 100$ mathematical layers. The exponential matrix is calculated using $N = 3$ order. A small value for $N$ is employed because of the large number of layers $N_L$ used to correctly calculate the curvature effects and the FGM law. The computational cost is acceptable because the dimension of the $E$ matrix is always $6 \times 6$ even if a layer wise approach is used and $N_L = 100$ mathematical layers are introduced. The values for $N$ and $N_L$ here adopted will be used for benchmarks proposed in Section 5.2.

After this preliminary assessment and considering all the further assessments proposed in the past authors' works [17]- [21], the present 3D exact shell solution can be considered as validated in the case of free vibration investigation of single-layered and multilayered FGM shell panels.

### 5.2 New benchmarks

Four different benchmarks are used in the present part to compare the 3D exact shell model, the 2D FE model and the classical and advanced 2D GDQ shell solutions. The first case is a single-layered FGM simply supported cylindrical shell having different thickness ratios $R_\alpha/h$ and $p$ coefficients for the FGM law. The second case is a sandwich cylindrical shell including two external classical skins and an internal FGM core, several thickness ratios $R_\alpha/h$ and $p$ coefficients for the FGM core are used. The third case is a single-layered FGM spherical shell having different thickness ratios $R_\alpha/h$ (the FGM law is the same already proposed in the first case). The last case considers a sandwich spherical shell having different thickness ratios $R_\alpha/h$ (the two external skins and the internal core have the same properties already described for the second case). Further details about these four different cases have already been proposed in Section 5.1.1 where the 2D FE method has been tested and validated. Further information can be found in Figure 3 and in Figure 4 for the geometries and FGM laws, respectively.

The mesh and the shell element to use in the FE results via Straus7, the Chebyshev-Gauss-Lobatto grid to use for 2D GDQ results and the order for the exponential matrix and the number of fictitious layers to use in the 3D exact results have been chosen by means of the validation procedures described in Section 5.1.

For all the proposed cases, the comparisons are made considering the first ten frequencies using the 2D FE code. The half-wave numbers $m$ and $n$ to impose in the $\alpha$ and $\beta$ directions are obtained via the graphical result of the first ten vibration modes. Therefore, these half-wave numbers have been introduced in the 3D exact shell model to calculate the same ten frequencies. For each ($m$,$n$) couple, the 3D exact shell model calculates infinite frequencies (from I to $\infty$). In the tables, in-plane modes have $w = 0$. There are some frequency values which are not calculated by the FE code. However, they have not been analyzed via the 3D exact shell model because this feature is not the main scope of the work. The scope of the present work is to remark the differences between the 2D computational methods and the 3D exact shell model for the first ten frequencies obtained via the 2D FE code. The classical and advanced 2D GDQ models do not use the half-wave numbers $m$ and $n$ for the frequency analyses because they are numerical methods with a certain number of degrees of freedom.

It is also fundamental to see the parameters which influence the differences between the various proposed models (e.g., geometries of the structure, laminations, materials, thickness ratios, vibration

modes and frequency orders).

The simply supported one-layered FGM cylindrical shell panel has been investigated in Tables 4-7 where four different exponents $p$ for the FGM law have been used ($p$ equals 0.0, 0.5, 1.0, 2.0, where $p$=0.0 means full ceramic material). In each table thin and thick structures are analyzed with the thickness ratio $R_\alpha/h$ from 1000 to 5. The first two columns show the first 10 frequencies calculated with the 2D FE model and the relative half-wave numbers $m$ and $n$ given by the FE visualization of the vibration modes. These half-wave numbers $m$ and $n$ have been used in the 3D exact model to calculate the same modes proposed by the 2D FE model. This mode order is specified in the third column for all 3D exact results. The last three columns give the GDQ results. The order of the 2D GDQ frequency is specified in an opportune column because sometimes the 2D FE model cannot give some results obtained by means of the 3D exact solution and the 2D GDQ models. In the case of one-layered structures, two different GDQ solutions are proposed, a GDQ-FSDT model based on the classical 2D Reissner-Mindilin model (the same used by the 2D shell element in the FE solution) and a GDQ-HOST model based on a fourth order of expansion in the thickness direction for each displacement component $u$, $v$ and $w$. In Table 4 the refined 2D GDQ-HOST model always gives the 3D exact solution for each thickness ratio $R_\alpha/h$ and for each eponent $p$ of the FGM law. The 2D FE model and the GDQ-FSDT solution use the same displacement model based on the Reissner-Mindilin hypothesis, however the GDQ-FSDT solution is always better than the 2D FE solution. The 2D FE solution gives larger errors for thick structures and/or higher order frequencies. In the case of in-plane vibration modes (those indicated with $w$=0 in parentheses), all the proposed models give correct results even if the structure is thick and the frequency has a higher order. This feature is due to the fact that the in-plane vibration modes satisfy the zero transverse normal strain hypothesis proposed in the Reissner-Mindlin model. All these considerations obtained from the Table 4 are also valid for Tables 5-7 where an exponent $p > 0$ is used for the FGM law. In these first four tables for the single-layered FGM cylindrical shell, the first ten frequencies obtained via the 2D FE solution are always the same first ten frequencies obtained via the 2D GDQ methods (the same vibration modes) as confirmed by the fifth column of the tables that indicates the order of frequencies in the GDQ solution. Figure 7 shows the vibration modes for the first four frequencies obtained in the case of one-layered FGM (with $p$=0.5) cylindrical shell panel with thickness ratio $R_\alpha/h$=5. The second frequency is an in-plane vibration mode (transverse displacement $w = 0$) as also confirmed by the results in Table 5. In Figure 7, the left part shows the vibration modes drawn via the 2D GDQ-HOST model and the right part shows the vibration modes drawn via the 3D exact shell solution. In the case of 3D exact shell solution, the vibration modes are given only via the evaluation of the three displacement components through the thickness direction $z$ because the behavior in the $\alpha$-$\beta$ plane is already known by means of the imposition of the half-wave numbers $m$ and $n$.

Sandwich cylindrical shell panels with simply-supported boundary conditions have been investigated in Tables 8-11. The structure in Table 8 has a classical core with properties that are a mean value between the top skin and bottom skin properties. Shells in Tables 9, 10 and 11 have an FGM core with exponential $p$ for the FGM law equals 0.5, 1.0 and 2.0, respectively. In each table, both thick and thin shells are analyzed (from thickness ratio $R_\alpha/h$=5 to $R_\alpha/h$=1000). The first ten frequencies calculated via the 2D FE model have been recalculated using the 3D exact model and several classical and advanced 2D GDQ models. The vibration modes calculated using the 2D FE model have been used to see the half-wave numbers $m$ and $n$ to impose in the 3D exact shell model. In Tables 8-11, the first ten vibration modes via 2D FE are the same first ten vibration modes via the 2D GDQ solutions. The differences in terms of frequency value depend on the frequency order and on the thickness ratio. 2D FE model is correct for thin shells and/or low frequency orders. 2D GDQ-FSDT model uses the same displacement model employed in the 2D FE model (the Reissner-Mindlin model) but it gives important improvements, for all the thickness ratios and vibration modes, with respect to the FE analysis. The 2D GDQ-HOST model always gives the exact 3D solution for each thickness

ratio, vibration mode and material configuration. 2D GDQ-ZZ model considers the addition of the Murakami zigzag function to the 2D GDQ-HOST model in order to recover the typical zigzag form of the displacement components due to the transverse anisotropy of the sandwich structures. However, these proposed sandwich structures do not have a significant transverse anisotropy (because of the FGM core) and for this reason 2D GDQ-ZZ model and 2D GDQ-HOST model are always coincident. The advantages of a zigzag model are more evident in the static analysis of sandwich structures with soft core because they have a strong transverse anisotropy [54], [55].

Tables 12-15 propose the free vibration investigation of simply supported single-layered FGM spherical shells. Spherical shells have a more complicated geometry because the presence of two radii of curvature gives a full coupling between all the three displacement components. For these reasons, the error between the 3D exact shell model and all the other 2D numerical models (FE and GDQ solutions) is bigger than the cylindrical shell cases. However, 2D GDQ solutions give a significant improvement with respect to the 2D FE models, in particular when a refined ESL model is used. In the spherical shell cases, in particular for thick structures, there is not a correspondence between the first ten vibration modes obtained via FEM and the first ten vibration modes obtained via GDQ method. This feature is clearly demonstrated by the frequency number indicated in the fifth column of Tables 12-15. For thick shells the 2D FE solution gives errors for the frequency value and for the vibration mode. 2D GDQ solution (in particular the refined ESL 2D GDQ solution) overcomes these limitations as clearly demonstrated by the comparison with the 3D exact model. However, some problems remain because the simply supported boundary conditions are very complicated to be imposed in spherical shell geometries by means of numerical methods. This feature is demonstrated by the fact that the FE and GDQ results are not symmetric even if the material is isotropic and the shell geometry is symmetric (see for example the different frequency values obtained for $m$=1 and $n$=2 and for $m$=2 and $n$=1 in Tables 12-15, actually these two frequency values must be equal as demonstrated by the 3D exact solution. This problem is common for several $m$ and $n$ values in Tables 12-15, and it is also evident in Tables 16-19 for sandwich spherical shells).

The free vibration investigation of simply supported sandwich spherical shells with classical and FGM cores is proposed in Tables 16-19, the 2D GDQ-ZZ model has been added with respect to the one-layered cases proposed in Tables 12-15. However, the proposed sandwich structures have a limited transverse anisotropy and for this reason the use of a refined ESL model is sufficient. The addition of the zigzag Murakami function does not give any advantage. All the considerations already proposed for the one-layered spherical shells of Tables 12-15 are still here valid. Figure 8 proposes the vibration modes for the first four frequencies obtained in the case of sandwich spherical shell panel with thickness ratio $R_\alpha/h$=10 and FGM core with $p$=1.0. The fourth frequency is an in-plane vibration mode as clearly demonstrated by the zero transverse displacement $w$ drawn through the thickness direction $z$. The multilayer configuration has bigger problems with the use of the 2D FE model, if compared to the same cases embedding only one FGM layer. The difficulties exhibited by the 2D FE solution are confirmed by the errors shown for the frequency values and for the vibration modes. The refined 2D GDQ models are the numerical theories closer to the 3D exact model.

# 6 Conclusions

Several refined and classical 2D GDQ methods and an exact 3D shell theory model have been used for the free vibration investigation of single-layered and sandwich cylindrical and spherical shell panels including FGM layers. 2D FE results have also been added for comparison purposes and to remark the improvements given by the GDQ methods with respect to the other numerical procedures.

The exact 3D shell model calculates infinite vibration modes from I to $\infty$ (for each possible combination of half-wave numbers $m$ and $n$). A 2D computational model (both FE and GDQ solutions) calculates a certain number of vibration modes because it has a certain number of global degrees of

freedom in the three directions $\alpha$, $\beta$ and $z$. A possible methodology to compare the 3D exact shell model with the numerical 2D theories is to obtain the frequencies using the 2D computational code (e.g., the 2D FE code) and then to calculate the 3D exact frequencies using the opportune half-wave numbers $m$ and $n$ (chosen via an appropriate vibration mode visualizations using the FE or GDQ solution). The 3D shell model could obtain some frequencies that are not calculated by the 2D computational models. However, this feature is not the main scope of this work and it could be the topic of a future companion paper. The present work explains the advantages and the limitations of 2D computational models. A classical 2D FE code uses a Reissner-Mindlin theory for the description of displacement components through the thickness direction. Results proposed in the present work confirm how the displacement model used by the commercial FE softwares could give significant errors for thick and moderately thick plates and shells, cumbersome FGM laws and multilayered configurations, higher frequency orders and some particular vibration modes. For all these features, refined 2D GDQ models are fundamental to obtain 3D exact frequencies. However, results given by the Reissner-Mindlin model solved by means of the GDQ method are more accurate than the same results obtained by the Reissner-Mindlin model solved via the FE solution. The 2D FE model could give errors in terms of frequency values and vibration mode evaluations, in particular for the cases of spherical shells, thick structures and/or multilayered configurations.

In conclusion, the use of advanced 2D GDQ theories is fundamental to obtain an improvement in the free vibration analysis of cylindrical and spherical shell panels embedding FGM layers and a quasi-3D description of complicated structures.

## References


[1] S. Brischetto, R. Leetsch, E. Carrera, T. Wallmersperger and B. Kröplin, Thermo-mechanical bending of functionally graded plates, *Journal of Thermal Stresses*, 31, 286-308, 2008.

[2] G. Mattei, A. Tirella and A. Ahluwalia, Functionally Graded Materials (FGMs) with predictable and controlled gradient profiles: computational modelling and realisation, *CMES: Computer Modeling in Engineering & Sciences*, 87, 483-504, 2012.

[3] V. Birman and L.W. Byrd, Modeling and analysis of functionally graded materials and structures, *Applied Mechanics Reviews*, 60, 195-216, 2007.

[4] L. Dong and S.N. Atluri, A simple procedure to develop efficient & stable hybrid/mixed elements, and Voronoi cell finite elements for macro- & micro-mechanics, *CMC: Computers Materials & Continua*, 24, 61-104, 2011.

[5] P.L. Bishay, J. Sladek, V. Sladek and S.N. Atluri, Analysis of functionally graded magneto-electro-elastic composites using hybrid/mixed finite elements and node-wise material properties, *CMC: Computers Materials & Continua*, 29, 213-262, 2012.

[6] P.L. Bishay and S.N. Atluri, High-performance 3D hybrid/mixed, and simple 3D Voronoi cell finite elements, for macro- & micro-mechanical modeling of solids, without using multi-field variational principles, *CMES: Computer Modeling in Engineering & Sciences*, 84, 41-97, 2012.

[7] S. Brischetto, Classical and mixed advanced models for sandwich plates embedding functionally graded cores, *Journal of Mechanics of Materials and Structures*, 4, 13-33, 2009.

[8] E. Carrera and S. Brischetto, A survey with numerical assessment of classical and refined theories for the analysis of sandwich plates, *Applied Mechanics Reviews*, 62, 1-17, 2009.

[9] F. Tornabene, N. Fantuzzi, F. Ubertini and E. Viola, Strong formulation finite element method based on differential quadrature: a survey, *Applied Mechanics Reviews*, 67, 020801-1-55.

[10] A. Alibeigloo and V. Nouri, Static analysis of functionally graded cylindrical shell with piezoelectric layers using differential quadrature method, *Composite Structures*, 92, 1775-1785, 2010.

[11] R. Akbari Alashti, M. Khorsand and M.H. Tarahhomi, Thermo-elastic analysis of a functionally graded spherical shell with piezoelectric layers by differential quadrature method, *Scientia Iranica*, 20, 109-119, 2013.

[12] A. Asanjarani, S. Satouri, A. Alizadeh and M.H. Kargarnovin, Free vibration analysis of 2D-FGM truncated conical shell resting on Winkler-Pasternak foundations based on FSDT, *Proceedings of the Institution of Mechanical Engineers, Part C: Journal of Mechanical Engineering Science*, 229, 818-839, 2015.

[13] R. Bahadori and M.M. Najafizadeh, Free vibration analysis of two-dimensional functionally graded axisymmetric cylindrical shell on Winkler-Pasternak elastic foundation by First-order Shear Deformation Theory and using Navier-differential quadrature solution methods, *Applied Mathematical Modelling* 39, 4877-4894, 2015.

[14] A. Jodaei, M. Jalal and M.H. Yas, Free vibration analysis of functionally graded annular plates by state-space based differential quadrature method and comparative modeling by ANN, *Composites Part B: Engineering*, 43, 340-353, 2012.

[15] Sh. Hosseini-Hashemi, H. Akhavan, H. Rokni Damavandi Taher, N. Daemi and A. Alibeigloo, Differential quadrature analysis of functionally graded circular and annular sector plates on elastic foundation, *Materials & Design*, 31, 1871-1880, 2010.

[16] L. Wu, H. Wang and D. Wang, Dynamic stability analysis of FGM plates by the moving least squares differential quadrature method, *Composite Structures*, 77, 383-394, 2007.

[17] S. Brischetto, Exact elasticity solution for natural frequencies of functionally graded simply-supported structures, *CMES: Computer Modeling in Engineering & Sciences*, 95, 391-430, 2013.

[18] S. Brischetto, Three-dimensional exact free vibration analysis of spherical, cylindrical, and flat one-layered panels, *Shock and Vibration*, Vol. 2014, Article ID 479738, 1-29, 2014.

[19] S. Brischetto, An exact 3D solution for free vibrations of multilayered cross-ply composite and sandwich plates and shells, *International Journal of Applied Mechanics*, 6, 1-42, 2014.

[20] S. Brischetto, A continuum elastic three-dimensional model for natural frequencies of single-walled carbon nanotubes, *Composites Part B: Engineering*, 61, 222-228, 2014.

[21] S. Brischetto, A continuum shell model including van der Waals interaction for free vibrations of double-walled carbon nanotubes, *CMES: Computer Modeling in Engineering & Sciences*, 104, 305-327, 2015.

[22] C.Y Dong, Three-dimensional free vibration analysis of functionally graded annular plates using the Chebyshev-Ritz method, *Materials and Design*, 29, 1518-1525. 2008.

[23] Q. Li, V.P. Iu and K.P. Kou, Three-dimensional vibration analysis of functionally graded material sandwich plates, *Journal of Sound and Vibration*, 311, 498-515, 2008.

[24] P. Malekzadeh, Three-dimensional free vibration analysis of thick functionally graded plates on elastic foundations, *Composite Structures*, 89, 367-373, 2009.

[25] S. Hosseini-Hashemi, H. Salehipour and S.R. Atashipour, Exact three-dimensional free vibration analysis of thick homogeneous plates coated by a functionally graded layer, *Acta Mechanica*, 223, 2153-2166, 2012.

[26] S.S. Vel and R.C. Batra, Three-dimensional exact solution for the vibration of functionally graded rectangular plates, *Journal of Sound and Vibration*, 272, 703-730, 2004.

[27] M. Kashtalyan, Three-dimensional elasticity solution for bending of functionally graded rectangular plates, *European Journal of Mechanics A/Solids*, 23, 853-864, 2004.

[28] Y. Xu and D. Zhou, Three-dimensional elasticity solution of functionally graded rectangular plates with variable thickness, *Composite Structures*, 91, 56-65, 2009.

[29] M. Kashtalyan and M. Menshykova, Three-dimensional elasticity solution for sandwich panels with a functionally graded core, *Composite Structures*, 87, 36-43, 2009.

[30] Z. Zhong and E.T. Shang, Three-dimensional exact analysis of a simply supported functionally gradient piezoelectric plate, *International Journal of Solids and Structures*, 40, 5335-5352, 2003.

[31] A. Alibeigloo, A.M. Kani and M.H. Pashaei, Elasticity solution for the free vibration analysis of functionally graded cylindrical shell bonded to thin piezoelectric layers, *International Journal of Pressure Vessels and Piping*, 89, 98-111, 2012.

[32] P. Zahedinejad, P. Malekzadeh, M. Farid and G. Karami, A semi-analytical three-dimensional free vibration analysis of functionally graded curved panels, *International Journal of Pressure Vessels and Piping*, 87, 470-480, 2010.

[33] W.Q. Chen, Z.G. Bian and H.J. Ding, Three-dimensional vibration analysis of fluid-filled orthotropic FGM cylindrical shells, *International Journal of Mechanical Sciences*, 46, 159-171, 2004

[34] S.S. Vel, Exact elasticity solution for the vibration of functionally graded anisotropic cylindrical shells, *Composite Structures*, 92, 2712-2727, 2010.

[35] J. Sladek, V. Sladek, J. Krivacek and C. Zhang, Meshless local Petrov-Galerkin method for stress and crack analysis in 3-D axisymmetric FGM bodies, *CMES: Computer Modeling in Engineering & Sciences*, 8, 259-270, 2005.

[36] J. Sladek, V. Sladek, C.L. Tan and S.N. Atluri, Analysis of transient heat conduction in 3D anisotropic functionally graded solids by the MLPG method, *CMES: Computer Modeling in Engineering & Sciences*, 32, 161-174, 2008.

[37] J. Sladek, V. Sladek and P. Solek, Elastic analysis in 3D anisotropic functionally graded solids by the MLPG, *CMES: Computer Modeling in Engineering & Sciences*, 43, 223-252, 2009.

[38] S. Brischetto and R. Torre, Exact 3D solutions and finite element 2D models for free vibration analysis of plates and cylinders, *Curved and Layered Structures*, 1, 59-92, 2014.

[39] F. Tornabene, S. Brischetto, N. Fantuzzi and E. Viola, Numerical and exact models for free vibration analysis of cylindrical and spherical shell panels, *Composites part B: Engineering*, 81, 231-250, 2015.

[40] S. Brischetto, F. Tornabene, N. Fantuzzi and E. Viola, 3D exact and 2D generalized differential quadrature models for free vibration analysis of functionally graded plates and cylinders, *Meccanica*, on-line, 1-40, 2016.

[41] S. Brischetto, F. Tornabene, N. Fantuzzi and M. Bacciocchi, Refined 2D and exact 3D shell models for the free vibration analysis of single- and double-walled carbon nanotubes, *Technologies*, 3, 259-284, 2015.

[42] Straus7, Straus7 Release 2.3.6 finite element analysis system. Sydney, Australia.

[43] F. Tornabene and E. Viola, Free vibration analysis of functionally graded panels and shells of revolution, *Meccanica*, 44, 255-281, 2009.

[44] F. Tornabene and E. Viola, Free vibrations of four-parameter functionally graded parabolic panels and shells of revolution, *European Journal of Mechanics - A/Solids*, 28, 991-1013, 2009.

[45] F. Tornabene, Free vibration analysis of functionally graded conical, cylindrical shell and annular plate structures with a four-parameter power-law distribution, *Computer Methods in Applied Mechanics and Engineering*, 198, 2911-2935, 2009.

[46] F. Tornabene, E. Viola and D.J. Inman, 2-D differential quadrature solution for vibration analysis of functionally graded conical, cylindrical shell and annular plate structures, *Journal of Sound & Vibration*, 328, 259-290, 2009.

[47] F. Tornabene, A. Liverani and G. Caligiana, FGM and laminated doubly-curved shells and panels of revolution with a free-form meridian: a 2-D GDQ solution for free vibrations, *International Journal of Mechanical Sciences*, 53, 446-470, 2011.

[48] F. Tornabene and A. Ceruti, Mixed static and dynamic optimizazion of four-parameter functionally graded completely doubly-curved and degenerate shells and panels using GDQ method, *Mathematical Problems in Engineering*, Vol. 2013, Article ID 867079, 1-33, 2013.

[49] E. Carrera, S. Brischetto and P. Nali, *Plates and Shells for Smart Structures: Classical and Advanced Theories for Modeling and Analysis*, John Wiley & Sons, Ltd., New Delhi, 2011.

[50] F. Tornabene, N. Fantuzzi and M. Bacciocchi, Free vibrations of free-form doubly-curved shells made of functionally graded materials using higher-order equivalent single layer theories, *Composites Part B: Engineering*, 67, 490-509, 2014.

[51] F. Tornabene, E. Viola and N. Fantuzzi, General higher-order equivalent single layer theory for free vibrations of doubly-curved laminated composite shells and panels, *Composite Structures*, 104, 94-117, 2013.

[52] F. Tornabene and E. Viola, Static analysis of functionally graded doubly-curved shells and panels of revolution, *Meccanica*, 48, 901-930, 2013.

[53] F. Tornabene and J.N. Reddy, FGM and laminated doubly-curved and degenerate shells resting on nonlinear elastic foundation: a GDQ solution for static analysis with a posteriori stress and strain recovery, *Journal of Indian Institute of Science*, 93, 635-688, 2013.

[54] F. Tornabene, N. Fantuzzi, E. Viola and R.C. Batra, Stress and strain recovery for functionally graded free-form and doubly-curved sandwich shells using higher-order equivalent single layer theory, *Composite Structures*, 119, 67-89, 2015.

[55] F. Tornabene, N. Fantuzzi, M. Bacciocchi and E. Viola, Accurate inter-laminar recovery for plates and doubly-curved shells with variable radii of curvature using layer-wise theories, *Composite Structures*, 124, 368-393, 2015.

[56] S. Brischetto and E. Carrera, Importance of higher order modes and refined theories in free vibration analysis of composite plates, *Journal of Applied Mechanics*, 77, 1-14, 2010.

[57] A.W. Leissa, *Vibration of Plates*, NASA SP-160, Washington, 1969.

[58] A.W. Leissa, *Vibration of Shells*, NASA SP-288, Washington, 1973.

[59] S. Werner, *Vibrations of Shells and Plates*, 3rd edition: revised and expanded, CRC Press, New York: Marcel Dekker Inc., 2004.

[60] W. Soedel, *Vibration of Shells and Plates*, Marcel Dekker, Inc., New York, 2005.

[61] F. Tornabene and N. Fantuzzi, *Mechanics of Laminated Composite Doubly-Curved Shell Structures. The Generalized Differential Quadrature Method and the Strong Formulation Finite Element Method*, Società Editrice Esculapio, Bologna (Italy), 2014.

[62] F.B. Hildebrand, E. Reissner and G.B. Thomas, *Notes on the Foundations of the Theory of Small Displacements of Orthotropic Shells*, NACA Technical Note No. 1833, Washington, 1949.

[63] G.B. Gustafson, *Systems of Differential Equations*, free available on http://www.math.utah.edu/gustafso/, accessed on 16th September 2014.

[64] W.E. Boyce and R.C. DiPrima, *Elementary Differential Equations and Boundary Value Problems*, John Wiley & Sons, Ltd., New York, 2001.

[65] D. Zwillinger, *Handbook of Differential Equations*, Academic Press, New York, 1997.

[66] C. Molery and C. Van Loan, Nineteen dubious ways to compute the exponential of a matrix, twenty-five years later, *SIAM Review*, 45, 1-46, 2003.

[67] A. Messina, Three dimensional free vibration analysis of cross-ply laminated plates through 2D and exact models, *3rd International Conference on Integrity, Reliability and Failure*, Porto (Portugal), 20-24 July 2009.

[68] K.P. Soldatos and J. Ye, Axisymmetric static and dynamic analysis of laminated hollow cylinders composed of monoclinic elastic layers, *Journal of Sound and Vibration*, 184, 245-259, 1995.

[69] F. Tornabene, General higher order layer-wise theory for free vibrations of doubly-curved laminated composite shells and panels, *Mechanics of Advanced Materials and Structures*, in press, 2015.

[70] F. Tornabene, N. Fantuzzi and M. Bacciocchi, Free vibrations of free-form doubly-curved shells made of functionally graded materials using higher-order equivalent single layer theories, *Composites Part B: Engineering*, 67, 490-509, 2014.

[71] F. Tornabene, N. Fantuzzi and M. Bacciocchi, The local GDQ method applied to general higher-order theories of doubly-curved laminated composite shells and panels: the free vibration analysis, *Composite Structures*, 116, 637-660, 2014.

[72] F. Tornabene, N. Fantuzzi, E. Viola and J.N. Reddy, Winkler-Pasternak foundation effect on the static and dynamic analyses of laminated doubly-curved and degenerate shells and panels, *Composites Part B: Engineering*, 57, 269-296, 2014.

[73] F. Tornabene, N. Fantuzzi, E. Viola and A.J.M. Ferreira, Radial basis function method applied to doubly-curved laminated composite shells and panels with a general higher-order equivalent single layer theory, *Composites Part B: Engineering*, 55, 642-659, 2013.

[74] F. Tornabene, *Meccanica delle Strutture a Guscio in Materiale Composito*, Società Editrice Esculapio, Bologna (Italy), 2012.

| | | $R_\alpha/h$=10 | | | $R_\alpha/h$=100 | | |
|---|---|---|---|---|---|---|---|
| Mesh | Elements | 2D FEM | 3D Exact | $\Delta$ | 2D FEM | 3D Exact | $\Delta$ |
| $5 \times 5$ | 25 | 61.63 | 56.25 | 9.56% | 26.06 | 20.39 | 27.8% |
| $7 \times 7$ | 49 | 58.88 | 56.25 | 4.68% | 23.07 | 20.39 | 13.1% |
| $15 \times 15$ | 225 | 57.04 | 56.25 | 1.40% | 20.96 | 20.39 | 2.79% |
| $20 \times 20$ | 400 | 56.83 | 56.25 | 1.03% | 20.68 | 20.39 | 1.42% |
| $40 \times 40$ | 1600 | 56.67 | 56.25 | 0.75% | 20.47 | 20.39 | 0.39% |
| $60 \times 60$ | 3600 | 56.65 | 56.25 | 0.71% | 20.43 | 20.39 | 0.20% |
| $80 \times 80$ | 6400 | 56.63 | 56.25 | 0.68% | 20.42 | 20.39 | 0.15% |
| $100 \times 100$ | 10000 | 56.62 | 56.25 | 0.66% | 20.41 | 20.39 | 0.10% |

Table 1: FE convergence study for the one-layered FGM ($p$=0.0) cylindrical shell panel. Comparison with the 3D frequency $f$ in $Hz$ for $m$=$n$=1 and $R_\alpha/h$=10, and for $m$=2 and $n$=1 and $R_\alpha/h$=100.

| | | $R_\alpha/h$=10 | | | $R_\alpha/h$=100 | | |
|---|---|---|---|---|---|---|---|
| Mesh | Elements | 2D FEM | 3D Exact | $\Delta$ | 2D FEM | 3D Exact | $\Delta$ |
| $5 \times 5$ | 25 | 167.1 | 133.0 | 25.6% | 107.7 | 89.08 | 20.9% |
| $7 \times 7$ | 49 | 150.9 | 133.0 | 13.5% | 97.22 | 89.08 | 9.14% |
| $15 \times 15$ | 225 | 140.9 | 133.0 | 5.94% | 90.81 | 89.08 | 1.94% |
| $20 \times 20$ | 400 | 139.9 | 133.0 | 5.19% | 90.09 | 89.08 | 1.13% |
| $40 \times 40$ | 1600 | 139.1 | 133.0 | 4.59% | 89.59 | 89.08 | 0.57% |
| $60 \times 60$ | 3600 | 138.9 | 133.0 | 4.44% | 89.49 | 89.08 | 0.46% |
| $80 \times 80$ | 6400 | 138.9 | 133.0 | 4.44% | 89.45 | 89.08 | 0.41% |
| $100 \times 100$ | 10000 | 138.9 | 133.0 | 4.44% | 89.44 | 89.08 | 0.40% |

Table 2: FE convergence study for the sandwich spherical shell panel with FGM ($p$=1.0) core. Comparison with the 3D frequency $f$ in $Hz$ for $m$=2 and $n$=1 and $R_\alpha/h$=10, and for $m$=1 and $n$=2 and $R_\alpha/h$=100.

| $p$ | 0.0 | 0.5 | 1.0 | 4.0 | 10 |
|---|---|---|---|---|---|
| | | | $a/R_\alpha$=0.5 | | |
| Reference 3D [32] | 0.2113 | 0.1814 | 0.1639 | 0.1367 | 0.1271 |
| Present 3D | 0.2129 | 0.1817 | 0.1638 | 0.1374 | 0.1296 |
| | | | $a/R_\alpha$=1.0 | | |
| Reference 3D [32] | 0.2164 | 0.1852 | 0.1676 | 0.1394 | 0.1286 |
| Present 3D | 0.2155 | 0.1848 | 0.1671 | 0.1392 | 0.1300 |

Table 3: Comparison between the 3D model based on the DQM by Zahedinejad et al. [32] and the present 3D exact solution. One-layered FGM cylindrical shell panel with thickness ratio $a/h$=5. Fundamental circular frequency $\bar{\omega} = \omega h \sqrt{\frac{\rho_c}{E_c}}$ for half-wave numbers $m$=$n$=1 and different radii of curvature $R_\alpha$ and exponents $p$ for the material law.

| 2D FEM | $m$,$n$ | mode | 3D Exact | freq. number | GDQ-FSDT | GDQ-HOST |
|---|---|---|---|---|---|---|
| $R_\alpha/h$=5 | | | | | | |
| 96.87 | 1,1 | I | 93.34 | 1 | 93.44 | 93.34 |
| 155.9 | 0,1 | I ($w$=0) | 155.0 | 2 | 155.0 | 155.0 |
| 176.5 | 1,2 | I | 167.2 | 3 | 167.1 | 167.2 |
| 290.7 | 1,3 | I | 264.0 | 4 | 263.2 | 264.0 |
| 296.1 | 1,0 | II ($w$=0) | 296.5 | 6 | 296.5 | 296.5 |
| 311.8 | 0,2 | II ($w$=0) | 310.1 | 7 | 310.1 | 310.1 |
| 333.4 | 2,1 | I | 290.9 | 5 | 288.7 | 290.9 |
| 344.5 | 1,1 | II ($w$=0) | 343.7 | 9 | 343.7 | 343.7 |
| 393.3 | 2,2 | I | 338.0 | 8 | 335.3 | 338.0 |
| 437.2 | 1,4 | I | 377.3 | 10 | 374.9 | 377.3 |
| $R_\alpha/h$=10 | | | | | | |
| 56.62 | 1,1 | I | 56.25 | 1 | 56.40 | 56.25 |
| 114.1 | 1,2 | I | 113.0 | 2 | 113.2 | 113.0 |
| 155.3 | 0,1 | II ($w$=0) | 155.1 | 3 | 155.0 | 155.0 |
| 174.9 | 2,1 | I | 167.4 | 4 | 167.0 | 167.4 |
| 179.2 | 1,3 | I | 175.2 | 5 | 175.3 | 175.2 |
| 210.5 | 2,2 | I | 200.2 | 6 | 199.8 | 200.2 |
| 257.0 | 1,4 | I | 246.0 | 7 | 245.8 | 246.1 |
| 270.8 | 2,3 | I | 254.8 | 8 | 254.2 | 254.8 |
| 296.1 | 1,0 | II ($w$=0) | 296.2 | 9 | 296.2 | 296.2 |
| 310.6 | 0,2 | II ($w$=0) | 310.1 | 10 | 310.1 | 310.1 |
| $R_\alpha/h$=100 | | | | | | |
| 20.41 | 2,1 | I | 20.39 | 1 | 20.40 | 20.39 |
| 32.67 | 1,1 | I | 32.66 | 2 | 32.66 | 32.66 |
| 39.74 | 3,1 | I | 39.67 | 3 | 39.67 | 39.67 |
| 39.87 | 2,2 | I | 39.84 | 4 | 39.85 | 39.84 |
| 46.27 | 3,2 | I | 46.19 | 5 | 46.20 | 46.19 |
| 59.55 | 3,3 | I | 59.43 | 6 | 59.45 | 59.43 |
| 65.86 | 2,3 | I | 65.79 | 7 | 65.81 | 65.79 |
| 69.9 | 4,1 | I | 69.68 | 8 | 69.67 | 69.68 |
| 74.07 | 4,2 | I | 73.83 | 9 | 73.83 | 73.83 |
| 77.21 | 3,4 | I | 77.03 | 10 | 77.05 | 77.03 |
| $R_\alpha/h$=1000 | | | | | | |
| 6.132 | 3,1 | I | 6.116 | 1 | 6.117 | 6.117 |
| 7.490 | 4,1 | I | 7.473 | 2 | 7.474 | 7.474 |
| 10.23 | 2,1 | I | 10.21 | 3 | 10.21 | 10.21 |
| 11.04 | 5,1 | I | 11.02 | 4 | 11.02 | 11.02 |
| 12.57 | 4,2 | I | 12.54 | 5 | 12.54 | 12.54 |
| 13.11 | 5,2 | I | 13.07 | 6 | 13.07 | 13.07 |
| 15.74 | 6,1 | I | 15.70 | 7 | 15.70 | 15.70 |
| 16.74 | 6,2 | I | 16.68 | 8 | 16.68 | 16.68 |
| 17.73 | 3,2 | I | 17.70 | 9 | 17.70 | 17.70 |
| 18.60 | 5,3 | I | 18.53 | 10 | 18.53 | 18.53 |

Table 4: Simply supported one-layered FGM cylindrical shell panel with $p$=0.0. Frequencies $f$ in $Hz$ for different thickness ratios $R_\alpha/h$.

| 2D FEM | $m$,$n$ | mode | 3D Exact | freq. number | GDQ-FSDT | GDQ-HOST |
|---|---|---|---|---|---|---|
| $R_\alpha/h$=5 | | | | | | |
| 83.81 | 1,1 | I | 78.94 | 1 | 78.84 | 78.93 |
| 135.2 | 0,1 | II ($w$=0) | 140.9 | 2 | 140.9 | 140.9 |
| 152.2 | 1,2 | I | 143.3 | 3 | 143.1 | 143.3 |
| 248.9 | 1,3 | I | 226.8 | 4 | 225.7 | 226.8 |
| 264.8 | 1,0 | II ($w$=0) | 262.9 | 6 | 262.9 | 262.9 |
| 270.4 | 0,2 | II ($w$=0) | 281.7 | 7 | 281.7 | 281.7 |
| 287.9 | 2,1 | I | 245.7 | 5 | 242.9 | 245.6 |
| 308.0 | 1,1 | II ($w$=0) | 306.0 | 9 | 306.0 | 306.0 |
| 338.8 | 2,2 | I | 287.1 | 8 | 283.8 | 287.0 |
| 371.8 | 1,4 | I | 324.9 | 10 | 322.2 | 324.8 |
| $R_\alpha/h$=10 | | | | | | |
| 49.00 | 1,1 | I | 48.35 | 1 | 48.43 | 48.34 |
| 99.27 | 1,2 | I | 98.23 | 2 | 98.37 | 98.22 |
| 136.7 | 0,1 | II ($w$=0) | 139.9 | 3 | 139.9 | 139.9 |
| 149.4 | 2,1 | I | 140.9 | 4 | 140.3 | 140.9 |
| 155.0 | 1,3 | I | 151.5 | 5 | 151.5 | 151.5 |
| 179.7 | 2,2 | I | 169.2 | 6 | 168.6 | 169.2 |
| 220.3 | 1,4 | I | 211.6 | 7 | 211.3 | 211.6 |
| 230.9 | 2,3 | I | 216.4 | 8 | 215.5 | 216.3 |
| 264.8 | 1,0 | II ($w$=0) | 263.9 | 9 | 263.9 | 263.9 |
| 273.5 | 0,2 | II ($w$=0) | 279.2 | 10 | 277.1 | 278.4 |
| $R_\alpha/h$=100 | | | | | | |
| 17.47 | 2,1 | I | 17.49 | 1 | 17.49 | 17.48 |
| 29.17 | 1,1 | I | 29.21 | 2 | 29.21 | 29.20 |
| 33.55 | 3,1 | I | 33.54 | 3 | 33.53 | 33.54 |
| 35.09 | 2,2 | I | 35.11 | 4 | 35.12 | 35.11 |
| 39.36 | 3,2 | I | 39.35 | 5 | 39.35 | 39.35 |
| 51.23 | 3,3 | I | 51.21 | 6 | 51.22 | 51.21 |
| 58.33 | 2,3 | I | 58.34 | 7 | 58.35 | 58.34 |
| 58.97 | 4,1 | I | 58.88 | 8 | 58.85 | 58.87 |
| 62.55 | 4,2 | I | 62.46 | 9 | 62.44 | 62.45 |
| 66.92 | 3,4 | I | 66.87 | 10 | 66.87 | 66.86 |
| $R_\alpha/h$=1000 | | | | | | |
| 5.354 | 3,1 | I | 5.352 | 1 | 5.351 | 5.351 |
| 6.361 | 4,1 | I | 6.369 | 2 | 6.368 | 6.368 |
| 9.131 | 2,1 | I | 9.128 | 3 | 9.127 | 9.127 |
| 9.318 | 5,1 | I | 9.330 | 4 | 9.329 | 9.329 |
| 11.03 | 4,2 | I | 11.01 | 5 | 11.01 | 11.01 |
| 11.23 | 5,2 | I | 11.22 | 6 | 11.22 | 11.22 |
| 13.27 | 6,1 | I | 13.28 | 7 | 13.27 | 13.28 |
| 14.17 | 6,2 | I | 14.17 | 8 | 14.17 | 14.17 |
| 15.81 | 3,2 | I | 15.79 | 9 | 15.79 | 15.79 |
| 16.24 | 5,3 | I | 16.22 | 10 | 16.21 | 16.21 |

Table 5: Simply supported one-layered FGM cylindrical shell panel with $p$=0.5. Frequencies $f$ in $Hz$ for different thickness ratios $R_\alpha/h$.

| 2D FEM | $m$,$n$ | mode | 3D Exact | freq. number | GDQ-FSDT | GDQ-HOST |
|---|---|---|---|---|---|---|
| $R_\alpha/h$=5 | | | | | | |
| 76.70 | 1,1 | I | 71.05 | 1 | 70.95 | 71.05 |
| 123.2 | 0,1 | II ($w$=0) | 131.6 | 3 | 131.7 | 131.7 |
| 138.9 | 1,2 | I | 129.8 | 2 | 129.6 | 129.8 |
| 226,2 | 1,3 | I | 205.2 | 4 | 204.4 | 205.2 |
| 245.3 | 1,0 | II ($w$=0) | 242.1 | 6 | 242.2 | 242.1 |
| 246.4 | 0,2 | II ($w$=0) | 263.0 | 8 | 263.0 | 263.0 |
| 262.7 | 2,1 | I | 220.2 | 5 | 217.8 | 220.2 |
| 285.3 | 1,1 | II ($w$=0) | 282.4 | 9 | 282.3 | 282.4 |
| 308.5 | 2,2 | I | 257.9 | 7 | 255.3 | 257.9 |
| 336.3 | 1,4 | I | 293.9 | 10 | 291.9 | 293.9 |
| $R_\alpha/h$=10 | | | | | | |
| 44.82 | 1,1 | I | 43.93 | 1 | 43.99 | 43.93 |
| 90.98 | 1,2 | I | 89.70 | 2 | 89.83 | 89.70 |
| 125.7 | 0,1 | II ($w$=0) | 130.1 | 4 | 130.1 | 130.1 |
| 135.8 | 2,1 | I | 126.5 | 3 | 126.0 | 126.5 |
| 141.6 | 1,3 | I | 137.9 | 5 | 138.0 | 137.9 |
| 163,3 | 2,2 | I | 152.2 | 6 | 151.6 | 152.2 |
| 200.5 | 1,4 | I | 192.0 | 7 | 191.8 | 192.0 |
| 209.7 | 2,3 | I | 194.9 | 8 | 194.2 | 194.9 |
| 245.3 | 1,0 | II ($w$=0) | 243.6 | 9 | 243.7 | 243.6 |
| 251.4 | 0,2 | II ($w$=0) | 260.1 | 10 | 250.1 | 251.2 |
| $R_\alpha/h$=100 | | | | | | |
| 15.90 | 2,1 | I | 15.87 | 1 | 15.87 | 15.87 |
| 27.01 | 1,1 | I | 27.03 | 2 | 27.03 | 27.03 |
| 30.35 | 3,1 | I | 30.24 | 3 | 30.23 | 30.24 |
| 32.31 | 2,2 | I | 32.28 | 4 | 32.29 | 32.28 |
| 35.73 | 3,2 | I | 35.61 | 5 | 35.61 | 35.61 |
| 46.73 | 3,3 | I | 46.60 | 6 | 46.60 | 46.60 |
| 53.33 | 4,1 | I | 53.05 | 7 | 53.03 | 53.05 |
| 53.84 | 2,3 | I | 53.78 | 8 | 53.80 | 53.78 |
| 56.60 | 4,2 | I | 56.31 | 9 | 56.29 | 56.31 |
| 61.22 | 3,4 | I | 61.05 | 10 | 61.06 | 61.05 |
| $R_\alpha/h$=1000 | | | | | | |
| 4.913 | 3,1 | I | 4.905 | 1 | 4.904 | 4.904 |
| 5.769 | 4,1 | I | 5.764 | 2 | 5.763 | 5.763 |
| 8.426 | 5,1 | I | 8.417 | 3 | 8.417 | 8.417 |
| 8.453 | 2,1 | I | 8.443 | 4 | 8.443 | 8.443 |
| 10.14 | 4,2 | I | 10.11 | 5 | 10.11 | 10.11 |
| 10.22 | 5,2 | I | 10.19 | 6 | 10.19 | 10.19 |
| 11.99 | 6,1 | I | 11.97 | 7 | 11.97 | 11.97 |
| 12.84 | 6,2 | I | 12.81 | 8 | 12.81 | 12.81 |
| 14.62 | 3,2 | I | 14.60 | 9 | 14.60 | 14.60 |
| 14.91 | 5,3 | I | 14.86 | 10 | 14.86 | 14.86 |

Table 6: Simply supported one-layered FGM cylindrical shell panel with $p$=1.0. Frequencies $f$ in $Hz$ for different thickness ratios $R_\alpha/h$.

| 2D FEM | $m$,$n$ | mode | 3D Exact | freq. number | GDQ-FSDT | GDQ-HOST |
|---|---|---|---|---|---|---|
| $R_\alpha/h$=5 | | | | | | |
| 70.45 | 1,1 | I | 64.07 | 1 | 64.08 | 64.07 |
| 109.9 | 0,1 | II ($w$=0) | 119.9 | 3 | 119.9 | 119.9 |
| 126.9 | 1,2 | I | 116.9 | 2 | 117.1 | 116.9 |
| 206.0 | 1,3 | I | 184.3 | 4 | 184.5 | 184.3 |
| 219.8 | 0,2 | II ($w$=0) | 239.2 | 8 | 239.3 | 239.2 |
| 221.8 | 1,0 | II ($w$=0) | 217.6 | 6 | 217.7 | 217.7 |
| 241.1 | 2,1 | I | 196.7 | 5 | 196.0 | 196.7 |
| 257.9 | 1,1 | II ($w$=0) | 254.2 | 9 | 254.2 | 254.2 |
| 282.5 | 2,2 | I | 230.4 | 7 | 229.9 | 230.4 |
| 305.4 | 1,4 | I | 263.2 | 10 | 263.3 | 263.3 |
| $R_\alpha/h$=10 | | | | | | |
| 40.88 | 1,1 | I | 39.78 | 1 | 39.84 | 39.78 |
| 82.69 | 1,2 | I | 81.10 | 2 | 81.26 | 81.10 |
| 112.9 | 0,1 | II ($w$=0) | 118.0 | 4 | 118.0 | 118.0 |
| 124.4 | 2,1 | I | 114.2 | 3 | 114.0 | 114.2 |
| 128.8 | 1,3 | I | 124.6 | 5 | 124.8 | 124.6 |
| 149.5 | 2,2 | I | 137.4 | 6 | 137.2 | 137.4 |
| 182.4 | 1,4 | I | 173.3 | 7 | 173.5 | 173.3 |
| 191.7 | 2,3 | I | 175.8 | 8 | 175.8 | 175.9 |
| 221.8 | 1,0 | II ($w$=0) | 219.5 | 9 | 219.6 | 219.5 |
| 225.8 | 0,2 | II ($w$=0) | 235.8 | 10 | 226.3 | 226.3 |
| $R_\alpha/h$=100 | | | | | | |
| 14.48 | 2,1 | I | 14.41 | 1 | 14.42 | 14.41 |
| 24.42 | 1,1 | I | 24.41 | 2 | 24.41 | 24.41 |
| 27.70 | 3,1 | I | 27.51 | 3 | 27.51 | 27.51 |
| 29.28 | 2,2 | I | 29.21 | 4 | 29.21 | 29.21 |
| 32.57 | 3,2 | I | 32.37 | 5 | 32.37 | 32.37 |
| 42.51 | 3,3 | I | 42.28 | 6 | 42.30 | 42.29 |
| 48.69 | 4,1 | I | 48.27 | 7 | 48.27 | 48.27 |
| 48.74 | 2,3 | I | 48.62 | 8 | 48.63 | 48.62 |
| 51.66 | 4,2 | I | 51.23 | 9 | 51.23 | 51.23 |
| 55.62 | 3,4 | I | 55.34 | 10 | 55.36 | 55.34 |
| $R_\alpha/h$=1000 | | | | | | |
| 4.457 | 3,1 | I | 4.443 | 1 | 4.442 | 4.442 |
| 5.257 | 4,1 | I | 5.241 | 2 | 5.241 | 5.241 |
| 7.643 | 2,1 | I | 7.625 | 3 | 7.626 | 7.625 |
| 7.687 | 5,1 | I | 7.662 | 4 | 7.662 | 7.662 |
| 9.190 | 4,2 | I | 9.154 | 5 | 9.154 | 9.154 |
| 9.300 | 5,2 | I | 9.259 | 6 | 9.259 | 9.259 |
| 10.94 | 6,1 | I | 10.90 | 7 | 10.90 | 10.90 |
| 11.70 | 6,2 | I | 11.65 | 8 | 11.65 | 11.65 |
| 13.23 | 3,2 | I | 13.19 | 9 | 13.19 | 13.19 |
| 13.53 | 5,3 | I | 13.46 | 10 | 13.46 | 13.46 |

Table 7: Simply supported one-layered FGM cylindrical shell panel with $p$=2.0. Frequencies $f$ in $Hz$ for different thickness ratios $R_\alpha/h$.

| 2D FEM | $m$,$n$ | mode | 3D Exact | freq. number | GDQ-FSDT | GDQ-HOST | GDQ-ZZ |
|---|---|---|---|---|---|---|---|
| | | | $R_\alpha/h$=5 | | | | |
| 54.70 | 1,1 | I | 51.41 | 1 | 51.45 | 51.42 | 51.42 |
| 86.25 | 0,1 | II ($w$=0) | 88.27 | 2 | 88.27 | 88.27 | 88.27 |
| 99.17 | 1,2 | I | 92.81 | 3 | 92.84 | 92.84 | 92.84 |
| 162.7 | 1,3 | I | 146.7 | 4 | 146.4 | 146.8 | 146.8 |
| 167.8 | 1,0 | II ($w$=0) | 166.4 | 6 | 166.4 | 166.4 | 166.4 |
| 172.5 | 0,2 | II ($w$=0) | 176.5 | 7 | 176.5 | 176.5 | 176.5 |
| 188.6 | 2,1 | I | 159.6 | 5 | 158.6 | 159.7 | 159.7 |
| 195.3 | 1,1 | II ($w$=0) | 193.4 | 9 | 193.4 | 193.4 | 193.4 |
| 222.0 | 2,2 | I | 186.1 | 8 | 184.9 | 186.2 | 186.2 |
| 243.8 | 1,4 | I | 209.7 | 10 | 208.9 | 209.9 | 209.9 |
| | | | $R_\alpha/h$=10 | | | | |
| 31.81 | 1,1 | I | 31.32 | 1 | 31.39 | 31.32 | 31.32 |
| 64.08 | 1,2 | I | 63.24 | 2 | 63.35 | 63.25 | 63.25 |
| 86.95 | 0,1 | II ($w$=0) | 88.07 | 3 | 88.07 | 88.07 | 88.07 |
| 98.07 | 2,1 | I | 92.19 | 4 | 92.00 | 92.21 | 92.21 |
| 100.5 | 1,3 | I | 97.83 | 5 | 97.91 | 97.84 | 97.84 |
| 117.9 | 2,2 | I | 110.5 | 6 | 110.3 | 110.5 | 110.5 |
| 143.6 | 1,4 | I | 137.1 | 7 | 137.0 | 137.1 | 137.1 |
| 151.5 | 2,3 | I | 141.0 | 8 | 140.8 | 141.0 | 141,0 |
| 167.8 | 1,0 | II ($w$=0) | 167.0 | 9 | 167.0 | 167.0 | 167.0 |
| 173.9 | 0,2 | II ($w$=0) | 176.1 | 10 | 176.1 | 176.1 | 176.1 |
| | | | $R_\alpha/h$=100 | | | | |
| 11.39 | 2,1 | I | 11.37 | 1 | 11.37 | 11.37 | 11.37 |
| 18.50 | 1,1 | I | 18.51 | 2 | 18.51 | 18.51 | 18.51 |
| 22.08 | 3,1 | I | 21.99 | 3 | 21.99 | 21.99 | 21.99 |
| 22.47 | 2,2 | I | 22.44 | 4 | 22.45 | 22.44 | 22.44 |
| 25.77 | 3,2 | I | 25.68 | 5 | 25.68 | 25.68 | 25.68 |
| 33.29 | 3,3 | I | 33.18 | 6 | 33.19 | 33,18 | 33.18 |
| 37.19 | 2,3 | I | 37.15 | 7 | 37.16 | 37.15 | 37.15 |
| 38.18 | 4,1 | I | 38.61 | 8 | 38.61 | 38.61 | 38.61 |
| 41.15 | 4,2 | I | 40.93 | 9 | 40.93 | 40.93 | 40.93 |
| 43.27 | 3,4 | I | 43.13 | 10 | 43.15 | 43.13 | 43.13 |
| | | | $R_\alpha/h$=1000 | | | | |
| 3.444 | 3,1 | I | 3.436 | 1 | 3.436 | 3.436 | 3.436 |
| 4.167 | 4,1 | I | 4.157 | 2 | 4.157 | 4.157 | 4.157 |
| 5.792 | 2,1 | I | 5.785 | 3 | 5.785 | 5.785 | 5.785 |
| 6.129 | 5,1 | I | 6.113 | 4 | 6.113 | 6.113 | 6.113 |
| 7.074 | 4,2 | I | 7.054 | 5 | 7.054 | 7.054 | 7.054 |
| 7.312 | 5,2 | I | 7.288 | 6 | 7.289 | 7.288 | 7.288 |
| 8.735 | 6,1 | I | 8.706 | 7 | 8.706 | 8.706 | 8.706 |
| 9.300 | 6,2 | I | 9.266 | 8 | 9.266 | 9.266 | 9.266 |
| 10.04 | 3,2 | I | 10.02 | 9 | 10.02 | 10.02 | 10.02 |
| 10.45 | 5,3 | I | 10.41 | 10 | 10.41 | 10.41 | 10.41 |

Table 8: Simply supported sandwich cylindrical shell panel embedding classical core. Frequencies $f$ in $Hz$ for different thickness ratios $R_\alpha/h$.

| 2D FEM | $m$,$n$ | mode | 3D Exact | freq. number | GDQ-FSDT | GDQ-HOST | GDQ-ZZ |
|---|---|---|---|---|---|---|---|
| | | | $R_\alpha/h$=5 | | | | |
| 53.16 | 1,1 | I | 49.97 | 1 | 49.88 | 49.97 | 49.97 |
| 86.55 | 0,1 | II ($w$=0) | 89.54 | 2 | 89.54 | 89.54 | 89.54 |
| 96.63 | 1,2 | I | 91.02 | 3 | 90.79 | 91.02 | 91.02 |
| 157.8 | 1,3 | I | 144.1 | 4 | 143.3 | 144.1 | 144.1 |
| 170.0 | 1,0 | II ($w$=0) | 167.9 | 6 | 167.9 | 167.9 | 167.9 |
| 173.1 | 0,2 | II ($w$=0) | 179.1 | 7 | 179.1 | 179.1 | 179.1 |
| 182.3 | 2,1 | I | 155.8 | 5 | 154.0 | 155.9 | 155.9 |
| 197.7 | 1,1 | II ($w$=0) | 195.4 | 9 | 195.4 | 195.4 | 195.4 |
| 214.5 | 2,2 | I | 182.3 | 8 | 180.1 | 182.3 | 182.3 |
| 235.4 | 1,4 | I | 206.6 | 10 | 204.7 | 206.7 | 206.7 |
| | | | $R_\alpha/h$=10 | | | | |
| 31.16 | 1,1 | I | 30.69 | 1 | 30.74 | 30.69 | 30.69 |
| 63.27 | 1,2 | I | 62.56 | 2 | 62.62 | 62.56 | 62.56 |
| 87.69 | 0,1 | II ($w$=0) | 89.30 | 4 | 89.30 | 89.30 | 89.30 |
| 94.50 | 2,1 | I | 89.05 | 3 | 88.66 | 89.05 | 89.05 |
| 98.60 | 1,3 | I | 96.35 | 5 | 96.32 | 96.35 | 96.35 |
| 113.7 | 2,2 | I | 107.0 | 6 | 106.6 | 107.0 | 107.0 |
| 139.9 | 1,4 | I | 134.4 | 7 | 134.1 | 134.4 | 134.4 |
| 146.1 | 2,3 | I | 137.0 | 8 | 136.4 | 137.0 | 137.0 |
| 170.0 | 1,0 | II ($w$=0) | 168.9 | 9 | 168.9 | 168.9 | 168.9 |
| 175.4 | 0,2 | II ($w$=0) | 178.6 | 10 | 175.5 | 176.5 | 176.5 |
| | | | $R_\alpha/h$=100 | | | | |
| 11.09 | 2,1 | I | 11.07 | 1 | 11.07 | 11.07 | 11.07 |
| 18.73 | 1,1 | I | 18.74 | 2 | 18.74 | 18.74 | 18.74 |
| 21.21 | 3,1 | I | 21.14 | 3 | 21.14 | 21.14 | 21.14 |
| 22.44 | 2,2 | I | 22.42 | 4 | 22.43 | 22.42 | 22.42 |
| 24.94 | 3,2 | I | 24.86 | 5 | 24.87 | 24.86 | 24.86 |
| 32.56 | 3,3 | I | 32.48 | 6 | 32.48 | 32.48 | 32.48 |
| 37.27 | 4,1 | I | 37.10 | 7 | 37.08 | 37.10 | 37.10 |
| 37.37 | 2,3 | I | 37.33 | 8 | 37.34 | 37.33 | 37.33 |
| 39.55 | 4,2 | I | 39.37 | 9 | 39.36 | 39.37 | 39.37 |
| 42.62 | 3,4 | I | 42.51 | 10 | 42.51 | 42.51 | 42.51 |
| | | | $R_\alpha/h$=1000 | | | | |
| 3.417 | 3,1 | I | 3.410 | 1 | 3.410 | 3.409 | 3.409 |
| 4.029 | 4,1 | I | 4.022 | 2 | 4.022 | 4.022 | 4.022 |
| 5.860 | 2,1 | I | 5.854 | 3 | 5.854 | 5.854 | 5.854 |
| 5.892 | 5,1 | I | 5.880 | 4 | 5.880 | 5.880 | 5.880 |
| 7.045 | 4,2 | I | 7.027 | 5 | 7.027 | 7.026 | 7.026 |
| 7.126 | 5,2 | I | 7.106 | 6 | 7.106 | 7.106 | 7.106 |
| 8.387 | 6,1 | I | 8.365 | 7 | 8.364 | 8.364 | 8.364 |
| 8.969 | 6,2 | I | 8.942 | 8 | 8.941 | 8.941 | 8.941 |
| 10.14 | 3,2 | I | 10.12 | 9 | 10.12 | 10.12 | 10.12 |
| 10.37 | 5,3 | I | 10.33 | 10 | 10.33 | 10.33 | 10.33 |

Table 9: Simply supported sandwich cylindrical shell panel embedding FGM core with $p$=0.5. Frequencies $f$ in $Hz$ for different thickness ratios $R_\alpha/h$.

| 2D FEM | $m$,$n$ | mode | 3D Exact | freq. number | GDQ-FSDT | GDQ-HOST | GDQ-ZZ |
|---|---|---|---|---|---|---|---|
| | | | $R_\alpha/h$=5 | | | | |
| 53.36 | 1,1 | I | 49.72 | 1 | 49.67 | 49.73 | 49.73 |
| 84.87 | 0,1 | II ($w$=0) | 88.51 | 2 | 88.51 | 88.51 | 88.51 |
| 96.65 | 1,2 | I | 90.34 | 3 | 90.24 | 90.34 | 90.34 |
| 157.8 | 1,3 | I | 142.8 | 4 | 142.4 | 142.8 | 142.8 |
| 167.8 | 1,0 | II ($w$=0) | 165.3 | 6 | 165.3 | 165.3 | 165.3 |
| 169.8 | 0,2 | II ($w$=0) | 177.0 | 7 | 177.0 | 177.0 | 177.0 |
| 183.3 | 2,1 | I | 154.3 | 5 | 153.2 | 154.3 | 154.3 |
| 195.2 | 1,1 | II ($w$=0) | 192.5 | 9 | 192.5 | 192.5 | 192.5 |
| 215.4 | 2,2 | I | 180.3 | 8 | 179.0 | 180.3 | 180.3 |
| 235.3 | 1,4 | I | 204.4 | 10 | 203.3 | 204.4 | 204.4 |
| | | | $R_\alpha/h$=10 | | | | |
| 31.10 | 1,1 | I | 30.54 | 1 | 30.59 | 30.54 | 30.54 |
| 62.93 | 1,2 | I | 62.09 | 2 | 62.16 | 62.09 | 62.09 |
| 86.27 | 0,1 | II ($w$=0) | 88.20 | 3 | 88.20 | 88.20 | 88.20 |
| 94.91 | 2,1 | I | 88.80 | 4 | 88.51 | 88.81 | 88.81 |
| 98.22 | 1,3 | I | 95.67 | 5 | 95.68 | 95.67 | 95.67 |
| 114.1 | 2,2 | I | 106.6 | 6 | 106.4 | 106.7 | 106.7 |
| 139.6 | 1,4 | I | 133.5 | 7 | 133.4 | 133.5 | 133.5 |
| 146.5 | 2,3 | I | 136.4 | 8 | 136.0 | 136.4 | 136.4 |
| 167.8 | 1,0 | II ($w$=0) | 166.5 | 9 | 166.5 | 166.5 | 166.5 |
| 172.6 | 0,2 | II ($w$=0) | 176.4 | 10 | 174.9 | 175.5 | 175.5 |
| | | | $R_\alpha/h$=100 | | | | |
| 11.07 | 2,1 | I | 11.04 | 1 | 11.04 | 11.04 | 11.04 |
| 18.49 | 1,1 | I | 18.50 | 2 | 18.50 | 18.50 | 18.50 |
| 21.25 | 3,1 | I | 21.16 | 3 | 21.16 | 21.16 | 21.16 |
| 22.24 | 2,2 | I | 22.21 | 4 | 22.22 | 22.21 | 22,21 |
| 24.93 | 3,2 | I | 24.84 | 5 | 24.84 | 24.84 | 24.84 |
| 32.46 | 3,3 | I | 32.35 | 6 | 32.36 | 32.35 | 32.35 |
| 36.96 | 2,3 | I | 36.92 | 7 | 36.93 | 36.92 | 36.92 |
| 37.35 | 4,1 | I | 37.14 | 8 | 37.13 | 37.14 | 37.14 |
| 39.62 | 4,2 | I | 39.40 | 9 | 39.40 | 39.41 | 39.41 |
| 42.40 | 3,4 | I | 42.26 | 10 | 42.27 | 42.26 | 42.26 |
| | | | $R_\alpha/h$=1000 | | | | |
| 3.392 | 3,1 | I | 3.384 | 1 | 3.384 | 3.384 | 3.384 |
| 4.028 | 4,1 | I | 4.020 | 2 | 4.020 | 4.020 | 4.020 |
| 5.786 | 2,1 | I | 5.779 | 3 | 5.779 | 5.779 | 5.779 |
| 5.900 | 5,1 | I | 5.887 | 4 | 5.887 | 5.887 | 5.887 |
| 6.986 | 4,2 | I | 6.966 | 5 | 6.966 | 6.966 | 6.966 |
| 7.108 | 5,2 | I | 7.087 | 6 | 7.087 | 7.087 | 7.087 |
| 8.403 | 6,1 | I | 8.377 | 7 | 8.377 | 8.377 | 8.377 |
| 8.974 | 6,2 | I | 8.944 | 8 | 8.943 | 8.943 | 8.943 |
| 10.02 | 3,2 | I | 9.997 | 9 | 9.997 | 9.997 | 9.997 |
| 10.29 | 5,3 | I | 10.25 | 10 | 10.25 | 10.25 | 10.25 |

Table 10: Simply supported sandwich cylindrical shell panel embedding FGM core with $p$=1.0. Frequencies $f$ in $Hz$ for different thickness ratios $R_\alpha/h$.

| 2D FEM | $m$,$n$ | mode | 3D Exact | freq. number | GDQ-FSDT | GDQ-HOST | GDQ-ZZ |
|---|---|---|---|---|---|---|---|
| | | | $R_\alpha/h$=5 | | | | |
| 54.12 | 1,1 | I | 49.90 | 1 | 49.97 | 49.91 | 49.91 |
| 83.17 | 0,1 | II ($w$=0) | 87.25 | 2 | 87.25 | 87.25 | 87.25 |
| 97.56 | 1,2 | I | 90.16 | 3 | 90.38 | 90.17 | 90.17 |
| 159.4 | 1,3 | I | 142.1 | 4 | 142.5 | 142.1 | 142.1 |
| 165.2 | 1,0 | II ($w$=0) | 162.4 | 6 | 162.4 | 162.4 | 162.4 |
| 166.4 | 0,2 | II ($w$=0) | 174.5 | 7 | 174.5 | 174.5 | 174.5 |
| 186.5 | 2,1 | I | 153.6 | 5 | 153.7 | 153.6 | 153.6 |
| 192.2 | 1,1 | II ($w$=0) | 189.3 | 9 | 189.3 | 189.3 | 189.3 |
| 218.9 | 2,2 | I | 179.1 | 8 | 179.5 | 179.1 | 179.1 |
| 237.8 | 1,4 | I | 201.7 | 10 | 203.3 | 202.7 | 202.7 |
| | | | $R_\alpha/h$=10 | | | | |
| 31.28 | 1,1 | I | 30.62 | 1 | 30.67 | 30.62 | 30.62 |
| 62.92 | 1,2 | I | 61.88 | 2 | 61.99 | 61.88 | 61.88 |
| 84.72 | 0,1 | II ($w$=0) | 86.87 | 3 | 86.87 | 86.87 | 86.87 |
| 96.50 | 2,1 | I | 89.50 | 4 | 89.44 | 89.51 | 89.51 |
| 98.52 | 1,3 | I | 95.49 | 5 | 95.63 | 95.49 | 95.49 |
| 115.9 | 2,2 | I | 107.3 | 6 | 107.4 | 107.3 | 107.3 |
| 140.6 | 1,4 | I | 133.5 | 7 | 133.7 | 133.5 | 133.5 |
| 148.7 | 2,3 | I | 136.9 | 8 | 137.0 | 136.9 | 136.9 |
| 165.2 | 1,0 | II ($w$=0) | 163.7 | 9 | 163.7 | 163.7 | 163.7 |
| 169.5 | 0,2 | II ($w$=0) | 173.7 | 10 | 173.7 | 173.7 | 173.7 |
| | | | $R_\alpha/h$=100 | | | | |
| 11.15 | 2,1 | I | 11.12 | 1 | 11.12 | 11.12 | 11.12 |
| 18.21 | 1,1 | I | 18.21 | 2 | 18.22 | 18.21 | 18.21 |
| 21.57 | 3,1 | I | 21.47 | 3 | 21.46 | 21.47 | 21.47 |
| 22.07 | 2,2 | I | 22.04 | 4 | 22.05 | 22.04 | 22.04 |
| 25.20 | 3,2 | I | 25.10 | 5 | 25.10 | 25.10 | 25.10 |
| 32.60 | 3,3 | I | 32.48 | 6 | 32.49 | 32.48 | 32.48 |
| 36.56 | 2,3 | I | 36.51 | 7 | 36.52 | 36.52 | 36.52 |
| 37.93 | 4,1 | I | 37.69 | 8 | 37.68 | 37.69 | 37.69 |
| 40.21 | 4,2 | I | 39.96 | 9 | 39.96 | 39.96 | 39.96 |
| 42.42 | 3,4 | I | 42.27 | 10 | 42.28 | 42.27 | 42.27 |
| | | | $R_\alpha/h$=1000 | | | | |
| 3.379 | 3,1 | I | 3.371 | 1 | 3.371 | 3.371 | 3.371 |
| 4.072 | 4,1 | I | 4.063 | 2 | 4.063 | 4.063 | 4.063 |
| 5.700 | 2,1 | I | 5.692 | 3 | 5.693 | 5.693 | 5.693 |
| 5.985 | 5,1 | I | 5.970 | 4 | 5.971 | 5.971 | 5.971 |
| 6.985 | 4,2 | I | 6.924 | 5 | 6.925 | 6.925 | 6.925 |
| 7.155 | 5,2 | I | 7.132 | 6 | 7.132 | 7.132 | 7.132 |
| 8.529 | 6,1 | I | 8.501 | 7 | 8.501 | 8.501 | 8.501 |
| 9.086 | 6,2 | I | 9.054 | 8 | 9.054 | 9.054 | 9.054 |
| 9.875 | 3,2 | I | 9.855 | 9 | 9.855 | 9.855 | 9.855 |
| 10.25 | 5,3 | I | 10.21 | 10 | 10.21 | 10.21 | 10.21 |

Table 11: Simply supported sandwich cylindrical shell panel embedding FGM core with $p$=2.0. Frequencies $f$ in $Hz$ for different thickness ratios $R_\alpha/h$.

| 2D FEM | $m$,$n$ | mode | 3D Exact | freq. number | GDQ-FSDT | GDQ-HOST |
|---|---|---|---|---|---|---|
| $R_\alpha/h$=5 | | | | | | |
| 205.3 | 1,1 | I | 201.9 | 1 | 201.5 | 200.4 |
| 273.0 | 0,1 | II ($w$=0) | 293.6 | 2 | 268.5 | 268.5 |
| 313.3 | 1,0 | II ($w$=0) | 293.6 | 3 | 307.5 | 307.6 |
| 412.7 | 2,1 | I | 359.9 | 4 | 361.9 | 362.8 |
| 413.1 | 1,2 | I | 359.9 | 5 | 363.1 | 363.9 |
| 440.1 | 1,1 | II ($w$=0) | 415.1 | 6 | 439.9 | 439.9 |
| 585.1 | 0,2 | II ($w$=0) | 586.8 | 8 | 575.0 | 575.0 |
| 620.2 | 2,0 | II ($w$=0) | 586.8 | 11 | 609.9 | 609.9 |
| 633.7 | 2,2 | I | 508.3 | 7 | 516.7 | 520.8 |
| 670.2 | 1,2 | II ($w$=0) | 655.9 | 12 | 661.8 | 661.8 |
| $R_\alpha/h$=10 | | | | | | |
| 167.0 | 1,1 | I | 167.8 | 1 | 167.4 | 166.8 |
| 254.3 | 1,2 | I | 245.4 | 2 | 247.0 | 246.4 |
| 254.4 | 2,1 | I | 245.4 | 3 | 247.1 | 246.4 |
| 271.4 | 0,1 | II ($w$=0) | 295.5 | 4 | 270.3 | 270.3 |
| 313.1 | 1,0 | II ($w$=0) | 295.5 | 5 | 311.7 | 311.7 |
| 368.7 | 2,2 | I | 337.8 | 6 | 346.2 | 346.2 |
| 435.7 | 1,3 | I | 400.4 | 7 | 401.9 | 402.4 |
| 443.3 | 3,1 | I | 400.4 | 8 | 406.7 | 407.4 |
| 446.3 | 1,1 | II ($w$=0) | 417.9 | 9 | 443.5 | 443.4 |
| 550.0 | 2,3 | I | 492.7 | 10 | 501.1 | 502.8 |
| $R_\alpha/h$=100 | | | | | | |
| 150.5 | 1,1 | I | 152.0 | 1 | 150.4 | 150.4 |
| 156.0 | 2,1 | I | 157.5 | 2 | 156.0 | 155.9 |
| 157.8 | 1,2 | I | 157.5 | 3 | 157.8 | 157.7 |
| 160.9 | 2,2 | I | 160.8 | 4 | 160.9 | 160.8 |
| 162.6 | 3,1 | I | 163.1 | 5 | 162.5 | 162.5 |
| 164.6 | 1,3 | I | 163.1 | 6 | 164.5 | 164.5 |
| 168.1 | 3,2 | I | 167.2 | 7 | 167.9 | 167.8 |
| 168.2 | 2,3 | I | 167.2 | 8 | 168.1 | 168.0 |
| 174.4 | 4,1 | I | 173.9 | 9 | 174.3 | 174.2 |
| 174.6 | 1,4 | I | 173.9 | 10 | 174.5 | 174.4 |
| $R_\alpha/h$=1000 | | | | | | |
| 149.5 | 1,1 | I | 151.9 | 1 | 149.4 | 149.4 |
| 155.9 | 2,1 | I | 156.2 | 2 | 154.4 | 154.4 |
| 157.2 | 1,2 | I | 156.2 | 3 | 155.5 | 155.5 |
| 157.9 | 2,2 | I | 157.3 | 4 | 156.6 | 156.6 |
| 159.3 | 3,1 | I | 157.7 | 5 | 156.7 | 156.7 |
| 159.9 | 3,2 | I | 157.1 | 6 | 157.5 | 157.5 |
| 160.5 | 1,3 | I | 157.7 | 7 | 157.7 | 157.7 |
| 160.7 | 4,1 | I | 158.4 | 8 | 157.8 | 157.8 |
| 161.3 | 2,3 | I | 157.1 | 9 | 157.9 | 157.9 |
| 162.3 | 1,4 | I | 158.6 | 12 | 158.5 | 158.5 |

Table 12: Simply supported one-layered FGM spherical shell panel with $p$=0.0. Frequencies $f$ in $Hz$ for different thickness ratios $R_\alpha/h$.

| 2D FEM | $m$,$n$ | mode | 3D Exact | freq. number | GDQ-FSDT | GDQ-HOST |
|---|---|---|---|---|---|---|
| $R_\alpha/h$=5 | | | | | | |
| 178.7 | 1,1 | I | 173.6 | 1 | 173.2 | 172.4 |
| 244.0 | 0,1 | II ($w$=0) | 264.6 | 2 | 242.1 | 242.1 |
| 279.8 | 1,0 | II ($w$=0) | 264.6 | 3 | 276.5 | 276.7 |
| 347.9 | 2,1 | I | 305.9 | 4 | 306.9 | 308.3 |
| 351.4 | 1,2 | I | 305.9 | 5 | 308.8 | 309.9 |
| 398.4 | 1,1 | II ($w$=0) | 374.2 | 6 | 396.6 | 396.6 |
| 521.9 | 0,2 | II ($w$=0) | 529.1 | 10 | 518.5 | 520.2 |
| 531.0 | 2,2 | I | 433.2 | 7 | 439.4 | 444.0 |
| 555.3 | 2,0 | II ($w$=0) | 529.1 | 11 | 550.0 | 549.9 |
| 598.4 | 1,2 | II ($w$=0) | 591.5 | 12 | 596.9 | 596.8 |
| $R_\alpha/h$=10 | | | | | | |
| 147.2 | 1,1 | I | 147.3 | 1 | 147.0 | 146.4 |
| 219.2 | 2,1 | I | 210.8 | 2 | 211.9 | 211.5 |
| 219.3 | 1,2 | I | 210.8 | 3 | 212.1 | 211.7 |
| 242.7 | 0,1 | II ($w$=0) | 265.4 | 4 | 242.7 | 242.7 |
| 279.7 | 1,0 | II ($w$=0) | 265.4 | 5 | 279.8 | 279.7 |
| 314.1 | 2,2 | I | 287.9 | 6 | 294.5 | 295.0 |
| 370.7 | 1,3 | I | 340.9 | 7 | 341.6 | 342.7 |
| 377.2 | 3,1 | I | 340.9 | 8 | 345.5 | 346.7 |
| 396.7 | 1,1 | II ($w$=0) | 375.3 | 9 | 398.1 | 398.1 |
| 472.4 | 2,3 | I | 419.4 | 10 | 425.7 | 428.0 |
| $R_\alpha/h$=100 | | | | | | |
| 134.1 | 1,1 | I | 135.9 | 1 | 134.5 | 134.4 |
| 138.1 | 2,1 | I | 140.7 | 2 | 139.3 | 139.3 |
| 141.1 | 1,2 | I | 140.7 | 3 | 140.9 | 140.9 |
| 143.2 | 3,1 | I | 145.3 | 5 | 144.8 | 144.7 |
| 143.9 | 2,2 | I | 143.4 | 4 | 143.5 | 143.4 |
| 146.7 | 1,3 | I | 145.3 | 6 | 146.6 | 146.5 |
| 149.5 | 2,3 | I | 148.7 | 8 | 149.4 | 149.3 |
| 149.7 | 3,2 | I | 148.7 | 7 | 149.1 | 149.1 |
| 152.9 | 4,1 | I | 154.0 | 9 | 154.3 | 154.2 |
| 164.7 | 1,4 | I | 154.0 | 10 | 154.5 | 154.5 |
| $R_\alpha/h$=1000 | | | | | | |
| 133.6 | 1,1 | I | 135.9 | 1 | 133.7 | 133.7 |
| 139.2 | 2,1 | I | 139.8 | 2 | 138.1 | 138.1 |
| 140.0 | 1,2 | I | 139.8 | 3 | 139.2 | 139.2 |
| 141.2 | 2,2 | I | 140.8 | 4 | 140.2 | 140.2 |
| 141.4 | 3,1 | I | 141.1 | 5 | 140.2 | 140.2 |
| 141.9 | 3,2 | I | 141.5 | 6 | 141.0 | 141.0 |
| 142.3 | 1,3 | I | 141.1 | 7 | 141.1 | 141.1 |
| 142.9 | 4,1 | I | 141.8 | 8 | 141.2 | 141.2 |
| 143.5 | 2,3 | I | 141.5 | 9 | 141.3 | 141.3 |
| 144.3 | 1,4 | I | 141.8 | 12 | 141.8 | 141.8 |

Table 13: Simply supported one-layered FGM spherical shell panel with $p$=0.5. Frequencies $f$ in $Hz$ for different thickness ratios $R_\alpha/h$.

| 2D FEM | $m$,$n$ | mode | 3D Exact | freq. number | GDQ-FSDT | GDQ-HOST |
|---|---|---|---|---|---|---|
| $R_\alpha/h$=5 | | | | | | |
| 163.8 | 1,1 | I | 157.4 | 1 | 157.2 | 156.3 |
| 226.0 | 0,1 | II ($w$=0) | 246.1 | 2 | 225.1 | 225.1 |
| 259.0 | 1,0 | II ($w$=0) | 246.1 | 3 | 256.5 | 256.7 |
| 312.8 | 1,2 | I | 275.0 | 5 | 278.7 | 279.4 |
| 319.7 | 2,1 | I | 275.0 | 4 | 276.2 | 277.2 |
| 369.6 | 1,1 | II ($w$=0) | 347.8 | 6 | 368.6 | 368.5 |
| 476.2 | 2,2 | I | 389.5 | 7 | 395.7 | 399.2 |
| 482.3 | 0,2 | II ($w$=0) | 491.2 | 10 | 481.5 | 481.4 |
| 514.5 | 2,0 | II ($w$=0) | 491.2 | 11 | 510.6 | 510.5 |
| 553.3 | 1,2 | II ($w$=0) | 548.8 | 12 | 553.9 | 553.7 |
| $R_\alpha/h$=10 | | | | | | |
| 135.0 | 1,1 | I | 135.1 | 1 | 134.8 | 134.3 |
| 200.0 | 2,1 | I | 191.1 | 2 | 192.1 | 191.7 |
| 200.3 | 1,2 | I | 191.1 | 3 | 192.4 | 192.0 |
| 224.8 | 0,1 | II ($w$=0) | 246.2 | 4 | 225.2 | 225.2 |
| 258.9 | 1,0 | II ($w$=0) | 246.2 | 5 | 259.6 | 259.5 |
| 285.2 | 2,2 | I | 259.9 | 6 | 265.8 | 266.2 |
| 335.8 | 1,3 | I | 307.2 | 7 | 308.1 | 309.0 |
| 343.2 | 3,1 | I | 307.2 | 8 | 311.5 | 312.5 |
| 366.1 | 1,1 | II ($w$=0) | 348.1 | 9 | 369.3 | 369.3 |
| 426.3 | 2,3 | I | 377.8 | 10 | 383.6 | 385.5 |
| $R_\alpha/h$=100 | | | | | | |
| 123.8 | 1,1 | I | 125.7 | 1 | 124.4 | 124.4 |
| 126.5 | 2,1 | I | 130.1 | 2 | 128.9 | 128.8 |
| 130.7 | 3,1 | I | 134.2 | 5 | 133.7 | 133.7 |
| 130.7 | 1,2 | I | 130.1 | 3 | 130.3 | 130.3 |
| 133.4 | 2,2 | I | 132.5 | 4 | 132.6 | 132.5 |
| 135.7 | 1,3 | I | 134.2 | 6 | 135.5 | 135.4 |
| 138.2 | 2,3 | I | 137.2 | 8 | 137.8 | 137.8 |
| 138.6 | 3,2 | I | 137.2 | 7 | 137.6 | 137.5 |
| 139.4 | 4,1 | I | 141.9 | 9 | 142.1 | 142.1 |
| 142.9 | 1,4 | I | 141.9 | 10 | 142.4 | 142.3 |
| $R_\alpha/h$=1000 | | | | | | |
| 123.7 | 1,1 | I | 125.8 | 1 | 123.8 | 123.8 |
| 128.5 | 2,1 | I | 129.4 | 2 | 127.9 | 127.9 |
| 129.0 | 1,2 | I | 129.4 | 3 | 128.8 | 128.8 |
| 130.0 | 2,2 | I | 130.3 | 4 | 129.7 | 129.7 |
| 130.5 | 3,1 | I | 130.6 | 5 | 129.8 | 129.8 |
| 131.0 | 3,2 | I | 131.0 | 6 | 130.5 | 130.5 |
| 131.4 | 1,3 | I | 130.6 | 7 | 130.6 | 130.6 |
| 131.8 | 4,1 | I | 131.2 | 8 | 130.7 | 130.7 |
| 131.9 | 2,3 | I | 131.0 | 9 | 130.8 | 130.7 |
| 133.4 | 1,4 | I | 131.4 | 12 | 131.3 | 131.3 |

Table 14: Simply supported one-layered FGM spherical shell panel with $p$=1.0. Frequencies $f$ in $Hz$ for different thickness ratios $R_\alpha/h$.

| 2D FEM | $m$,$n$ | mode | 3D Exact | freq. number | GDQ-FSDT | GDQ-HOST |
|---|---|---|---|---|---|---|
| $R_\alpha/h$=5 | | | | | | |
| 148.7 | 1,1 | I | 141.0 | 1 | 141.0 | 140.1 |
| 204.4 | 0,1 | II ($w$=0) | 223.3 | 2 | 204.3 | 204.3 |
| 234.1 | 1,0 | II ($w$=0) | 223.3 | 3 | 232.4 | 232.4 |
| 281.8 | 2,1 | I | 245.2 | 4 | 247.7 | 247.1 |
| 292.1 | 1,2 | I | 245.2 | 5 | 250.4 | 249.6 |
| 335.0 | 1,1 | II ($w$=0) | 315.2 | 6 | 334.1 | 333.8 |
| 428.6 | 2,2 | I | 346.1 | 7 | 355.0 | 354.7 |
| 435.0 | 0,2 | II ($w$=0) | 444.2 | 10 | 435.8 | 435.3 |
| 466.9 | 2,0 | II ($w$=0) | 444.2 | 11 | 461.9 | 461.4 |
| 499.5 | 1,2 | II ($w$=0) | 495.7 | 12 | 500.7 | 500.1 |
| $R_\alpha/h$=10 | | | | | | |
| 121.6 | 1,1 | I | 121.5 | 1 | 121.3 | 120.8 |
| 181.9 | 2,1 | I | 172.0 | 2 | 173.1 | 172.6 |
| 182.1 | 1,2 | I | 172.0 | 3 | 173.4 | 172.8 |
| 203.2 | 0,1 | II ($w$=0) | 222.9 | 4 | 203.9 | 203.9 |
| 234.0 | 1,0 | II ($w$=0) | 222.9 | 5 | 235.0 | 234.9 |
| 259.7 | 2,2 | I | 233.6 | 6 | 239.6 | 239.3 |
| 305.3 | 1,3 | I | 275.9 | 7 | 277.7 | 277.4 |
| 313.9 | 3,1 | I | 275.9 | 8 | 280.8 | 280.6 |
| 329.9 | 1,1 | II ($w$=0) | 315.1 | 9 | 334.2 | 334.1 |
| 386.8 | 2,3 | I | 338.7 | 10 | 345.7 | 345.7 |
| $R_\alpha/h$=100 | | | | | | |
| 111.5 | 1,1 | I | 113.5 | 1 | 112.3 | 112.2 |
| 113.2 | 2,1 | I | 117.4 | 2 | 116.3 | 116.3 |
| 116.7 | 3,1 | I | 121.2 | 5 | 120.7 | 120.7 |
| 118.3 | 1,2 | I | 117.4 | 3 | 117.6 | 117.6 |
| 120.8 | 2,2 | I | 119.6 | 4 | 119.7 | 119.7 |
| 122.7 | 1,3 | I | 121.2 | 6 | 122.3 | 122.2 |
| 124.7 | 4,1 | I | 128.2 | 9 | 128.4 | 128.4 |
| 125.1 | 2,3 | I | 123.9 | 8 | 124.5 | 124.4 |
| 125.5 | 3,2 | I | 123.9 | 7 | 124.3 | 124.2 |
| 129.4 | 1,4 | I | 128.2 | 10 | 128.7 | 128.6 |
| $R_\alpha/h$=1000 | | | | | | |
| 111.7 | 1,1 | I | 113.6 | 1 | 111.8 | 111.7 |
| 115.6 | 2,1 | I | 116.8 | 2 | 115.5 | 115.5 |
| 115.8 | 1,2 | I | 116.8 | 3 | 116.3 | 116.3 |
| 116.5 | 2,2 | I | 117.7 | 4 | 117.1 | 117.1 |
| 116.8 | 3,1 | I | 118.0 | 5 | 117.2 | 117.2 |
| 117.6 | 3,2 | I | 118.2 | 6 | 117.8 | 117.8 |
| 118.0 | 1,3 | I | 118.0 | 7 | 117.9 | 117.9 |
| 118.8 | 4,1 | I | 118.5 | 8 | 118.0 | 118.0 |
| 119.1 | 2,3 | I | 118.2 | 9 | 118.1 | 118.1 |
| 119.7 | 4.2 | I | 118.6 | 10 | 118.3 | 118.3 |

Table 15: Simply supported one-layered FGM spherical shell panel with $p$=2.0. Frequencies $f$ in $Hz$ for different thickness ratios $R_\alpha/h$.

| 2D FEM | $m$,$n$ | mode | 3D Exact | freq. number | GDQ-FSDT | GDQ-HOST | GDQ-ZZ |
|---|---|---|---|---|---|---|---|
| | | | $R_\alpha/h$=5 | | | | |
| 115.2 | 1,1 | I | 111.7 | 1 | 111.6 | 111.0 | 111.0 |
| 154.7 | 0,1 | II ($w$=0) | 165.6 | 2 | 151.4 | 151.4 | 151.4 |
| 117.5 | 1,0 | II ($w$=0) | 165.6 | 3 | 173.3 | 173.3 | 173.3 |
| 228.2 | 1,2 | I | 197.9 | 5 | 200.1 | 200.4 | 200.4 |
| 230.0 | 2,1 | I | 197.9 | 4 | 199.2 | 199.6 | 199.6 |
| 252.5 | 1,1 | II ($w$=0) | 234.1 | 6 | 248.1 | 248.1 | 248.1 |
| 331.1 | 0,2 | II ($w$=0) | 331.0 | 8 | 324.4 | 324.4 | 324.4 |
| 348.3 | 2,0 | II ($w$=0) | 331.0 | 11 | 344.1 | 344.1 | 344.1 |
| 353.5 | 2,2 | I | 279.6 | 7 | 284.9 | 286.7 | 286.7 |
| 379.5 | 1,2 | II ($w$=0) | 370.1 | 12 | 373.4 | 373.4 | 373.4 |
| | | | $R_\alpha/h$=10 | | | | |
| 94.07 | 1,1 | I | 94.09 | 1 | 93.83 | 93.51 | 93.51 |
| 142.2 | 1,2 | I | 136.2 | 3 | 137.2 | 136.9 | 136.9 |
| 142.3 | 2,1 | I | 136.2 | 2 | 137.1 | 136.8 | 136.8 |
| 153.8 | 0,1 | II ($w$=0) | 167.0 | 4 | 152.8 | 152.8 | 152.8 |
| 177.4 | 1,0 | II ($w$=0) | 167.0 | 5 | 176.1 | 176.1 | 176.1 |
| 205.3 | 2,2 | I | 186.9 | 6 | 191.6 | 191.5 | 191.5 |
| 242.6 | 1,3 | I | 221.3 | 7 | 222.4 | 222.6 | 222.6 |
| 246.9 | 3,1 | I | 221.3 | 8 | 225.0 | 225.2 | 225.2 |
| 252.1 | 1,1 | II ($w$=0) | 236.2 | 9 | 250.6 | 250.6 | 250.6 |
| 310.3 | 2,3 | I | 272.3 | 10 | 277.2 | 278.0 | 278.0 |
| | | | $R_\alpha/h$=100 | | | | |
| 85.11 | 1,1 | I | 86.10 | 1 | 85.19 | 85.17 | 85.17 |
| 87.88 | 2,1 | I | 89.17 | 2 | 88.30 | 88.29 | 88.29 |
| 89.43 | 1,2 | I | 89.17 | 3 | 89.31 | 89.29 | 89.29 |
| 91.27 | 2,2 | I | 90.96 | 4 | 91.01 | 90.99 | 90.99 |
| 91.39 | 3,1 | I | 92.26 | 5 | 91.90 | 91.87 | 91.87 |
| 93.15 | 1,3 | I | 92.26 | 6 | 93.06 | 93.03 | 93.03 |
| 95.12 | 2,3 | I | 94.50 | 8 | 94.96 | 94.92 | 94.92 |
| 95.16 | 3,2 | I | 94.50 | 7 | 94.84 | 94.80 | 94.80 |
| 97.92 | 4,1 | I | 98.13 | 9 | 98.31 | 98.27 | 98.27 |
| 98.61 | 1,4 | I | 98.13 | 10 | 98.44 | 98.39 | 98.39 |
| | | | $R_\alpha/h$=1000 | | | | |
| 84.69 | 1,1 | I | 86.06 | 1 | 84.68 | 84.67 | 84.67 |
| 88.41 | 2,1 | I | 88.52 | 2 | 87.48 | 87.48 | 87.48 |
| 88.86 | 1,2 | I | 88.52 | 3 | 88.14 | 88.14 | 88.14 |
| 89.57 | 2,2 | I | 89.16 | 4 | 88.76 | 88.76 | 88.76 |
| 89.68 | 3,1 | I | 89.38 | 5 | 88.80 | 88.80 | 88.80 |
| 90.15 | 3,2 | I | 89.59 | 6 | 89.28 | 89.28 | 89.28 |
| 90.42 | 1,3 | I | 89.38 | 7 | 89.34 | 89.34 | 89.34 |
| 90.82 | 4,1 | I | 89.78 | 8 | 89.44 | 89.44 | 89.44 |
| 91.22 | 2,3 | I | 89.59 | 9 | 89.46 | 89.46 | 89.46 |
| 91.28 | 1,4 | I | 89.78 | 12 | 89.84 | 89.83 | 89.83 |

Table 16: Simply supported spherical shell panel embedding classical core. Frequencies $f$ in $Hz$ for different thickness ratios $R_\alpha/h$.

| 2D FEM | $m$,$n$ | mode | 3D Exact | freq. number | GDQ-FSDT | GDQ-HOST | GDQ-ZZ |
|---|---|---|---|---|---|---|---|
| | | | $R_\alpha/h$=5 | | | | |
| 113.9 | 1,1 | I | 110.7 | 1 | 110.3 | 110.0 | 110.0 |
| 156.6 | 0,1 | II ($w$=0) | 167.4 | 2 | 153.1 | 153.1 | 153.1 |
| 179.6 | 1,0 | II ($w$=0) | 167.4 | 3 | 175.0 | 175.1 | 175.1 |
| 220.3 | 1,2 | I | 194.5 | 5 | 196.0 | 197.1 | 197.1 |
| 222.7 | 2,1 | I | 194.5 | 4 | 194.8 | 196.0 | 196.0 |
| 255.7 | 1,1 | II ($w$=0) | 236.8 | 6 | 250.9 | 250.9 | 250.9 |
| 334.9 | 0,2 | II ($w$=0) | 334.8 | 10 | 328.1 | 331.0 | 331.0 |
| 335.8 | 2,2 | I | 275.5 | 7 | 279.0 | 282.4 | 282.4 |
| 356.3 | 2,0 | II ($w$=0) | 334.8 | 11 | 348.0 | 348.0 | 348.0 |
| 384.1 | 1,2 | II ($w$=0) | 374.3 | 12 | 377.7 | 377.7 | 377.7 |
| | | | $R_\alpha/h$=10 | | | | |
| 94.17 | 1,1 | I | 94.32 | 1 | 94.01 | 93.70 | 93.70 |
| 139.4 | 2,1 | I | 134.1 | 2 | 134.7 | 134.6 | 134.6 |
| 139.5 | 1,2 | I | 134.1 | 3 | 134.9 | 134.8 | 134.8 |
| 155.8 | 0,1 | II ($w$=0) | 169.0 | 4 | 154.6 | 154.6 | 154.6 |
| 179.5 | 1,0 | II ($w$=0) | 169.0 | 5 | 178.2 | 178.2 | 178.2 |
| 199.1 | 2,2 | I | 182.9 | 6 | 186.9 | 187.4 | 187.4 |
| 234.8 | 1,3 | I | 216.4 | 7 | 216.7 | 217.6 | 217.6 |
| 239.0 | 3,1 | I | 216.4 | 8 | 219.2 | 220.1 | 220.1 |
| 254.5 | 1,1 | II ($w$=0) | 239.0 | 9 | 253.6 | 253.6 | 253.6 |
| 298.9 | 2,3 | I | 266.3 | 10 | 270.0 | 271.8 | 271.8 |
| | | | $R_\alpha/h$=100 | | | | |
| 86.07 | 1,1 | I | 87.22 | 1 | 86.28 | 86.26 | 86.26 |
| 88.50 | 2,1 | I | 90.26 | 2 | 89.38 | 89.36 | 89.36 |
| 90.56 | 1,2 | I | 90.26 | 3 | 90.39 | 90.38 | 90.38 |
| 91.66 | 3,1 | I | 93.16 | 5 | 92.79 | 92.76 | 92.76 |
| 92.37 | 2,2 | I | 91.96 | 4 | 91.99 | 91.97 | 91.97 |
| 94.08 | 1,3 | I | 93.16 | 6 | 93.98 | 93.95 | 93.95 |
| 95.85 | 2,3 | I | 95.23 | 8 | 95.67 | 95.63 | 95.63 |
| 95.96 | 3,2 | I | 95.23 | 7 | 95.52 | 95.49 | 95.49 |
| 97.72 | 4,1 | I | 98.58 | 9 | 98.71 | 98.67 | 98.67 |
| 99.07 | 1,4 | I | 98.58 | 10 | 98.88 | 98.85 | 98.85 |
| | | | $R_\alpha/h$=1000 | | | | |
| 85.77 | 1,1 | I | 87.20 | 1 | 85.80 | 85.79 | 85.79 |
| 89.38 | 2,1 | I | 89.69 | 2 | 88.64 | 88.64 | 88.64 |
| 89.85 | 1,2 | I | 89.69 | 3 | 89.31 | 89.31 | 89.31 |
| 90.67 | 2,2 | I | 90.34 | 4 | 89.93 | 89.93 | 89.93 |
| 90.93 | 3,1 | I | 90.56 | 5 | 89.98 | 89.98 | 89.98 |
| 91.08 | 3,2 | I | 90.78 | 6 | 90.45 | 90.45 | 90.45 |
| 91.24 | 1,3 | I | 90.56 | 7 | 90.52 | 90.52 | 90.52 |
| 91.56 | 4,1 | I | 90.97 | 12 | 91.00 | 91.00 | 91.00 |
| 92.13 | 2,3 | I | 90.78 | 9 | 90.64 | 90.64 | 90.64 |
| 92.78 | 1,4 | I | 90.97 | 8 | 90.62 | 90.62 | 90.62 |

Table 17: Simply supported spherical shell panel embedding FGM core with $p$=0.5. Frequencies $f$ in $Hz$ for different thickness ratios $R_\alpha/h$.

| 2D FEM | $m$,$n$ | mode | 3D Exact | freq. number | GDQ-FSDT | GDQ-HOST | GDQ-ZZ |
|---|---|---|---|---|---|---|---|
| $R_\alpha/h$=5 | | | | | | | |
| 113.2 | 1,1 | I | 109.3 | 1 | 109.0 | 108.5 | 108.5 |
| 154.6 | 0,1 | II ($w$=0) | 165.0 | 2 | 151.0 | 151.0 | 151.0 |
| 177.3 | 1,0 | II ($w$=0) | 165.0 | 3 | 172.5 | 172.6 | 172.6 |
| 219.0 | 1,2 | I | 191.9 | 5 | 194.0 | 194.5 | 194.5 |
| 222.8 | 2,1 | I | 191.9 | 4 | 192.9 | 193.5 | 193.5 |
| 252.9 | 1,1 | II ($w$=0) | 233.4 | 6 | 247.4 | 247.4 | 247.4 |
| 330.3 | 0,2 | II ($w$=0) | 330.1 | 9 | 322.9 | 323.4 | 323.4 |
| 334.3 | 2,2 | I | 271.2 | 7 | 276.3 | 278.0 | 278.0 |
| 352.4 | 2,0 | II ($w$=0) | 330.1 | 11 | 343.1 | 343.1 | 343.1 |
| 378.9 | 1,2 | II ($w$=0) | 369.1 | 12 | 372.4 | 372.4 | 372.4 |
| $R_\alpha/h$=10 | | | | | | | |
| 93.02 | 1,1 | I | 93.11 | 1 | 92.80 | 92.54 | 92.54 |
| 138.9 | 1,2 | I | 133.0 | 3 | 133.8 | 133.6 | 133.6 |
| 138.9 | 2,1 | I | 133.0 | 2 | 133.6 | 133.4 | 133.4 |
| 153.8 | 0,1 | II ($w$=0) | 166.7 | 4 | 152.5 | 152.5 | 152.5 |
| 177.2 | 1,0 | II ($w$=0) | 166.7 | 5 | 175.8 | 175.8 | 175.8 |
| 198.9 | 2,2 | I | 181.4 | 6 | 185.7 | 185.9 | 185.9 |
| 234.5 | 1,3 | I | 214.7 | 7 | 215.4 | 215.8 | 215.8 |
| 239.3 | 3,1 | I | 214.7 | 8 | 217.8 | 218.3 | 218.3 |
| 251.0 | 1,1 | II ($w$=0) | 235.8 | 9 | 250.1 | 250.1 | 250.1 |
| 298.4 | 2,3 | I | 264.0 | 10 | 268.4 | 269.4 | 269.4 |
| $R_\alpha/h$=100 | | | | | | | |
| 84.84 | 1,1 | I | 86.06 | 1 | 85.14 | 85.12 | 85.12 |
| 87.03 | 2,1 | I | 89.08 | 2 | 88.21 | 88.19 | 88.19 |
| 89.44 | 1,2 | I | 89.08 | 3 | 89.21 | 89.20 | 89.20 |
| 90.13 | 3,1 | I | 92.00 | 5 | 91.63 | 91.61 | 91.61 |
| 91.30 | 2,2 | I | 90.79 | 4 | 90.82 | 90.80 | 90.80 |
| 92.94 | 1,3 | I | 92.00 | 6 | 92.81 | 92.77 | 92.77 |
| 94.76 | 2,3 | I | 94.09 | 8 | 94.53 | 94.49 | 94.49 |
| 94.96 | 3,2 | I | 94.09 | 7 | 94.39 | 94.36 | 94.36 |
| 96.30 | 4,1 | I | 97.48 | 9 | 97.62 | 97.59 | 97.59 |
| 98.04 | 1,4 | I | 97.48 | 10 | 97.78 | 97.75 | 97.75 |
| $R_\alpha/h$=1000 | | | | | | | |
| 84.63 | 1,1 | I | 86.06 | 1 | 84.67 | 84.67 | 84.67 |
| 88.07 | 2,1 | I | 88.51 | 2 | 87.48 | 87.48 | 87.48 |
| 88.48 | 1,2 | I | 88.51 | 3 | 88.13 | 88.13 | 88.13 |
| 89.29 | 2,2 | I | 89.15 | 4 | 88.75 | 88.75 | 88.75 |
| 89.59 | 3,1 | I | 89.37 | 5 | 88.80 | 88.80 | 88.80 |
| 89.80 | 3,2 | I | 89.58 | 6 | 89.27 | 89.27 | 89.27 |
| 89.94 | 1,3 | I | 89.37 | 7 | 89.33 | 89.33 | 89.33 |
| 90.23 | 1,4 | I | 89.77 | 12 | 89.81 | 89.81 | 89.81 |
| 90.66 | 2,3 | I | 89.58 | 9 | 89.45 | 89.45 | 89.45 |
| 91.51 | 4,1 | I | 89.77 | 8 | 89.43 | 89.43 | 89.43 |

Table 18: Simply supported spherical shell panel embedding FGM core with $p$=1.0. Frequencies $f$ in $Hz$ for different thickness ratios $R_\alpha/h$.

| 2D FEM | $m$,$n$ | mode | 3D Exact | freq. number | GDQ-FSDT | GDQ-HOST | GDQ-ZZ |
|---|---|---|---|---|---|---|---|
| | | | $R_\alpha/h$=5 | | | | |
| 113.1 | 1,1 | I | 108.2 | 1 | 108.1 | 107.5 | 107.5 |
| 152.3 | 0,1 | II ($w$=0) | 162.4 | 2 | 148.5 | 148.5 | 148.5 |
| 174.7 | 1,0 | II ($w$=0) | 162.4 | 3 | 169.8 | 169.8 | 169.8 |
| 219.8 | 1,2 | I | 190.1 | 5 | 193.4 | 192.5 | 192.5 |
| 225.2 | 2,1 | I | 190.1 | 4 | 192.4 | 191.6 | 191.6 |
| 248.8 | 1,1 | II ($w$=0) | 229.6 | 6 | 243.3 | 243.3 | 243.3 |
| 325.1 | 0,2 | II ($w$=0) | 324.7 | 9 | 318.2 | 318.2 | 318.2 |
| 335.8 | 2,2 | I | 267.5 | 7 | 275.4 | 274.0 | 274.0 |
| 348.9 | 2,0 | II ($w$=0) | 324.7 | 11 | 337.5 | 337.5 | 337.5 |
| 372.9 | 1,2 | II ($w$=0) | 363.0 | 12 | 366.3 | 366.3 | 366.3 |
| | | | $R_\alpha/h$=10 | | | | |
| 91.98 | 1,1 | I | 91.94 | 1 | 91.67 | 91.38 | 91.38 |
| 139.3 | 1,2 | I | 132.5 | 2 | 133.4 | 133.0 | 133.0 |
| 139.4 | 2,1 | I | 132.5 | 3 | 133.5 | 133.1 | 133.1 |
| 151.4 | 0,1 | II ($w$=0) | 164.1 | 4 | 150.1 | 150.1 | 150.1 |
| 174.5 | 1,0 | II ($w$=0) | 164.1 | 5 | 173.0 | 173.0 | 173.0 |
| 200.6 | 2,2 | I | 181.1 | 6 | 186.0 | 185.6 | 185.6 |
| 236.6 | 1,3 | I | 214.2 | 7 | 215.9 | 215.4 | 215.4 |
| 242.1 | 3,1 | I | 214.2 | 8 | 218.4 | 217.9 | 217.9 |
| 247.3 | 1,1 | II ($w$=0) | 232.0 | 9 | 246.2 | 246.1 | 246.1 |
| 301.4 | 2,3 | I | 263.1 | 10 | 269.1 | 268.5 | 268.5 |
| | | | $R_\alpha/h$=100 | | | | |
| 83.45 | 1,1 | I | 84.69 | 1 | 83.79 | 83.77 | 83.77 |
| 85.50 | 2,1 | I | 87.69 | 2 | 86.84 | 86.82 | 86.82 |
| 88.11 | 1,2 | I | 87.69 | 3 | 87.83 | 87.82 | 87.82 |
| 88.64 | 3,1 | I | 90.69 | 5 | 90.35 | 90.32 | 90.32 |
| 90.03 | 2,2 | I | 89.44 | 4 | 89.49 | 89.46 | 89.46 |
| 91.65 | 1,3 | I | 90.69 | 6 | 91.49 | 91.46 | 91.46 |
| 93.58 | 2,3 | I | 92.87 | 7 | 93.20 | 93.16 | 93.16 |
| 93.81 | 3,2 | I | 92.87 | 8 | 93.32 | 93.28 | 93.28 |
| 95.07 | 4,1 | I | 96.39 | 9 | 96.56 | 96.52 | 96.52 |
| 96.98 | 1,4 | I | 96.39 | 10 | 96.69 | 96.65 | 96.65 |
| | | | $R_\alpha/h$=1000 | | | | |
| 83.29 | 1,1 | I | 84.69 | 1 | 83.33 | 83.33 | 83.33 |
| 86.57 | 2,1 | I | 87.11 | 2 | 86.09 | 86.09 | 86.09 |
| 86.96 | 1,2 | I | 87.11 | 3 | 86.74 | 86.74 | 86.74 |
| 87.72 | 2,2 | I | 87.74 | 4 | 87.35 | 87.35 | 87.35 |
| 88.06 | 3,1 | I | 87.96 | 5 | 87.39 | 87.39 | 87.39 |
| 88.29 | 3,2 | I | 88.17 | 6 | 87.86 | 87.85 | 87.85 |
| 88.50 | 1,3 | I | 87.96 | 7 | 87.92 | 87.92 | 87.92 |
| 88.76 | 1,4 | I | 88.35 | 12 | 88.40 | 88.40 | 88.40 |
| 89.06 | 2,3 | I | 88.17 | 9 | 88.04 | 88.04 | 88.04 |
| 89.97 | 4.2 | I | 88.35 | 10 | 88.25 | 88.25 | 88.25 |

Table 19: Simply supported spherical shell panel embedding FGM core with $p$=2.0. Frequencies $f$ in $Hz$ for different thickness ratios $R_\alpha/h$.

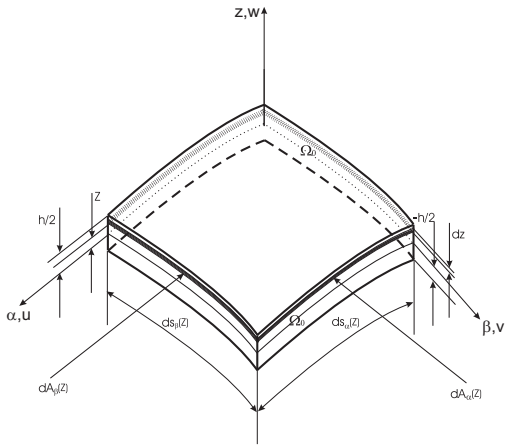


Figure 1: Reference system, geometrical parameters and notations for shells.

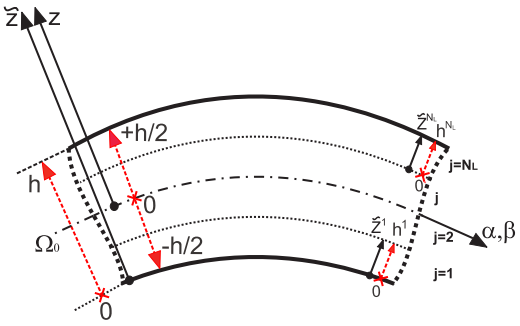


Figure 2: Thickness coordinates $z$ and $\tilde{z}$, and local/global reference systems for shells.

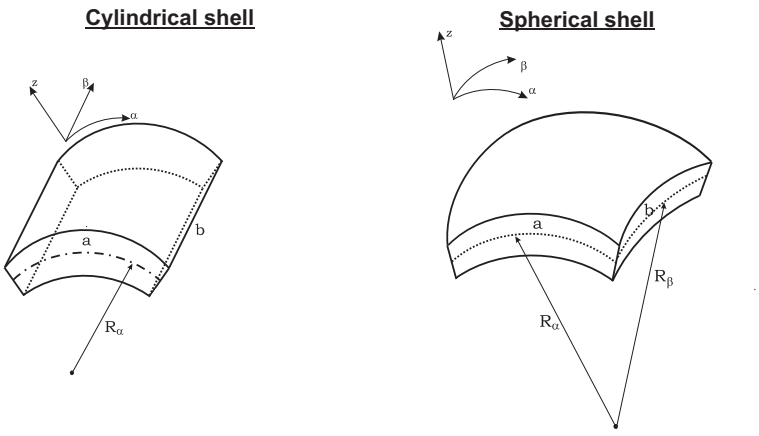


Figure 3: Cylindrical and spherical shell panel geometries for the validation of the FE model and for the new benchmarks.

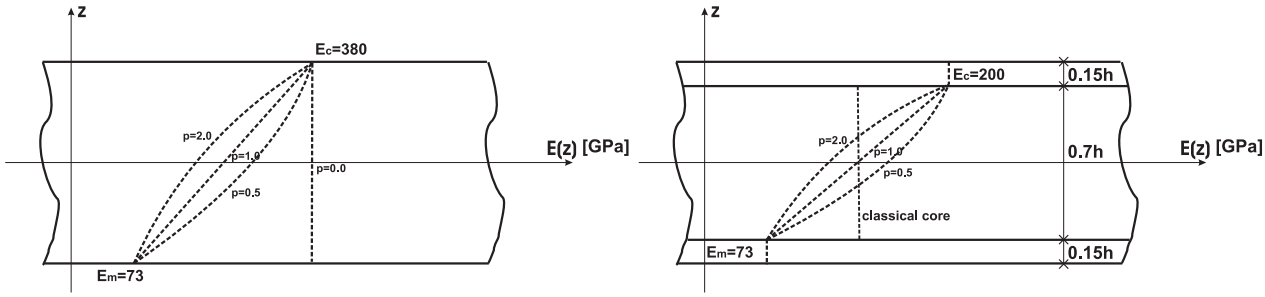


Figure 4: Functionally graded material law through the thickness direction of the one-layered cases and the sandwich cases.

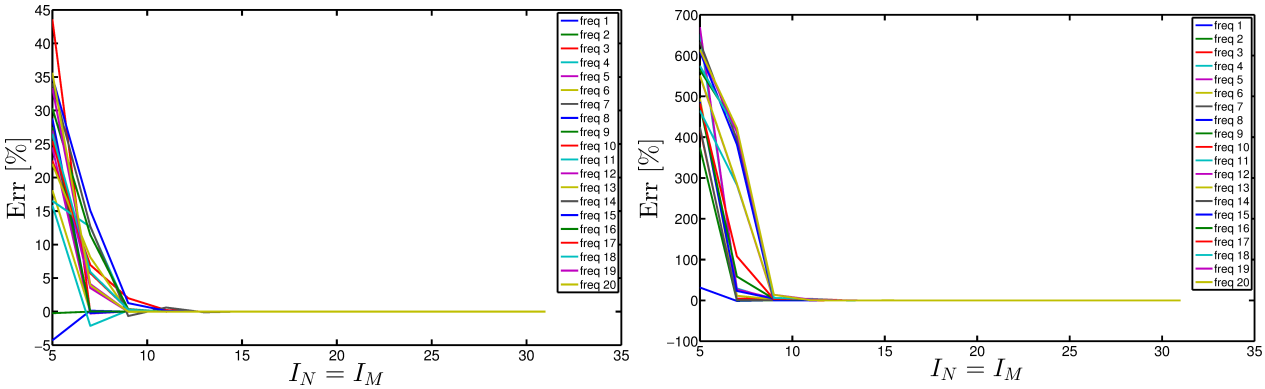


Figure 5: Convergence analysis of the 2D GDQ method for a sandwich cylindrical panel varying the number of grid points. Thickness values $h$=2$m$ and $h$=0.1$m$, respectively.

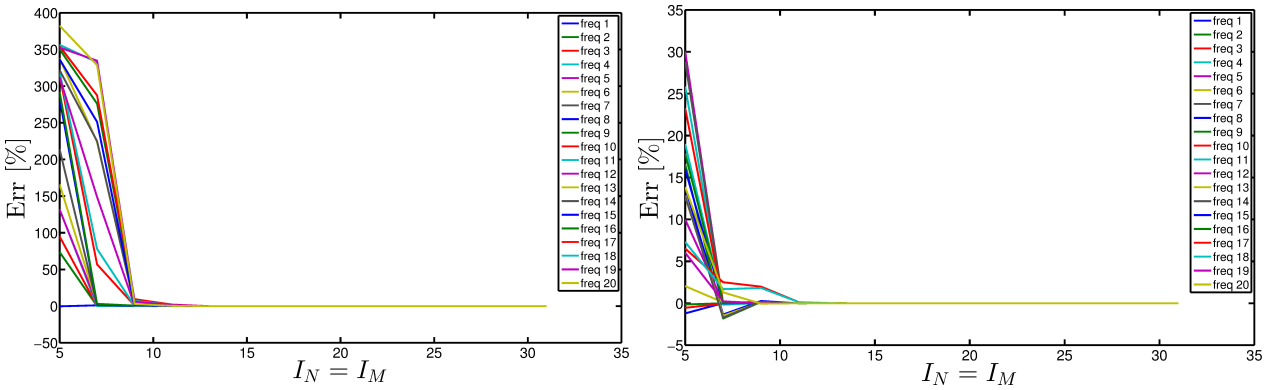


Figure 6: Convergence analysis of the 2D GDQ method for a sandwich spherical panel varying the number of grid points. Thickness values $h$=2$m$ and $h$=0.1$m$, respectively.

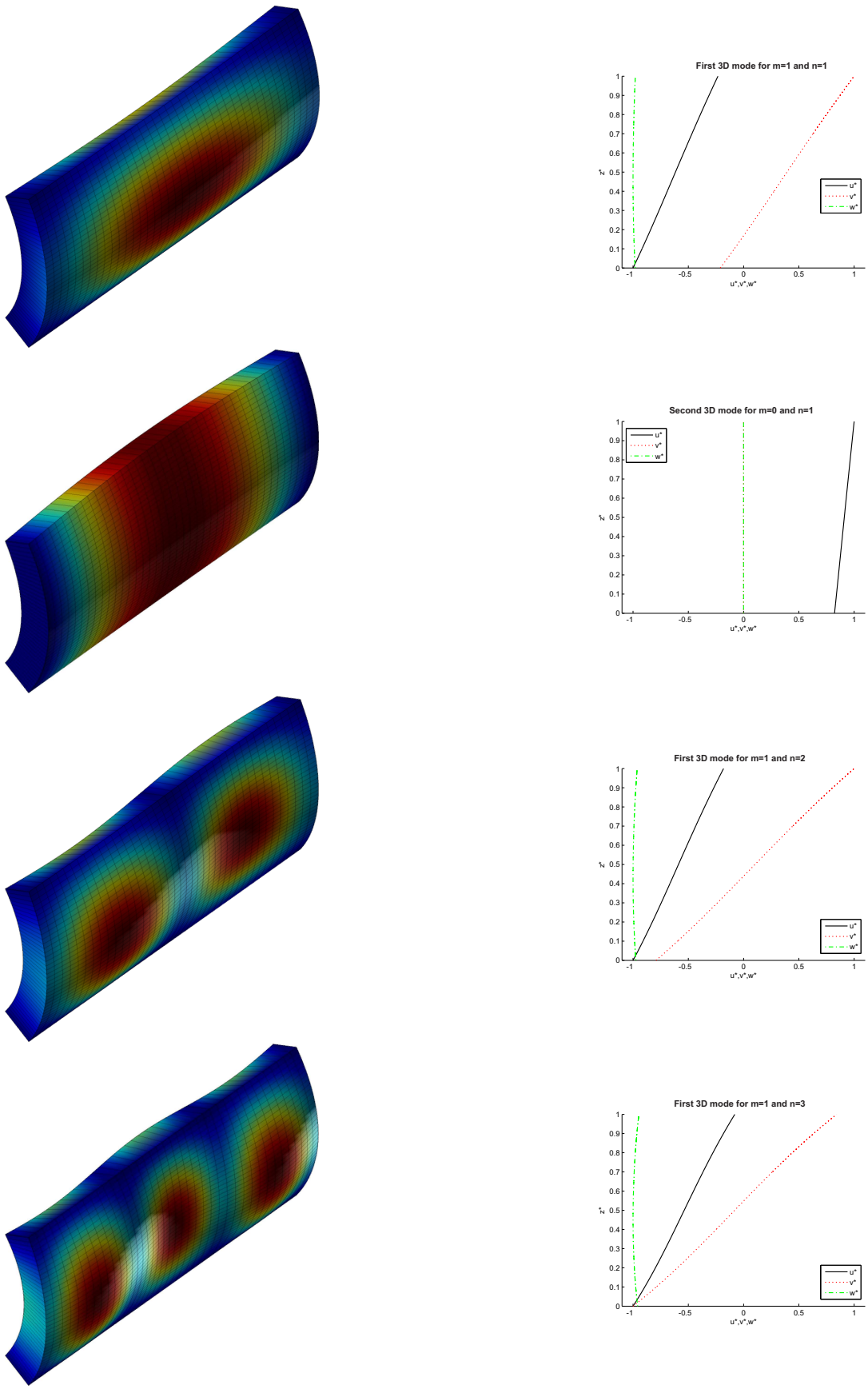


Figure 7: Simply supported one-layered FGM ($p$=0.5) cylindrical shell with thickness ratio $R_\alpha/h$=5. First four frequencies via 2D GDQ solution (on the left) and via 3D exact solution (on the right).

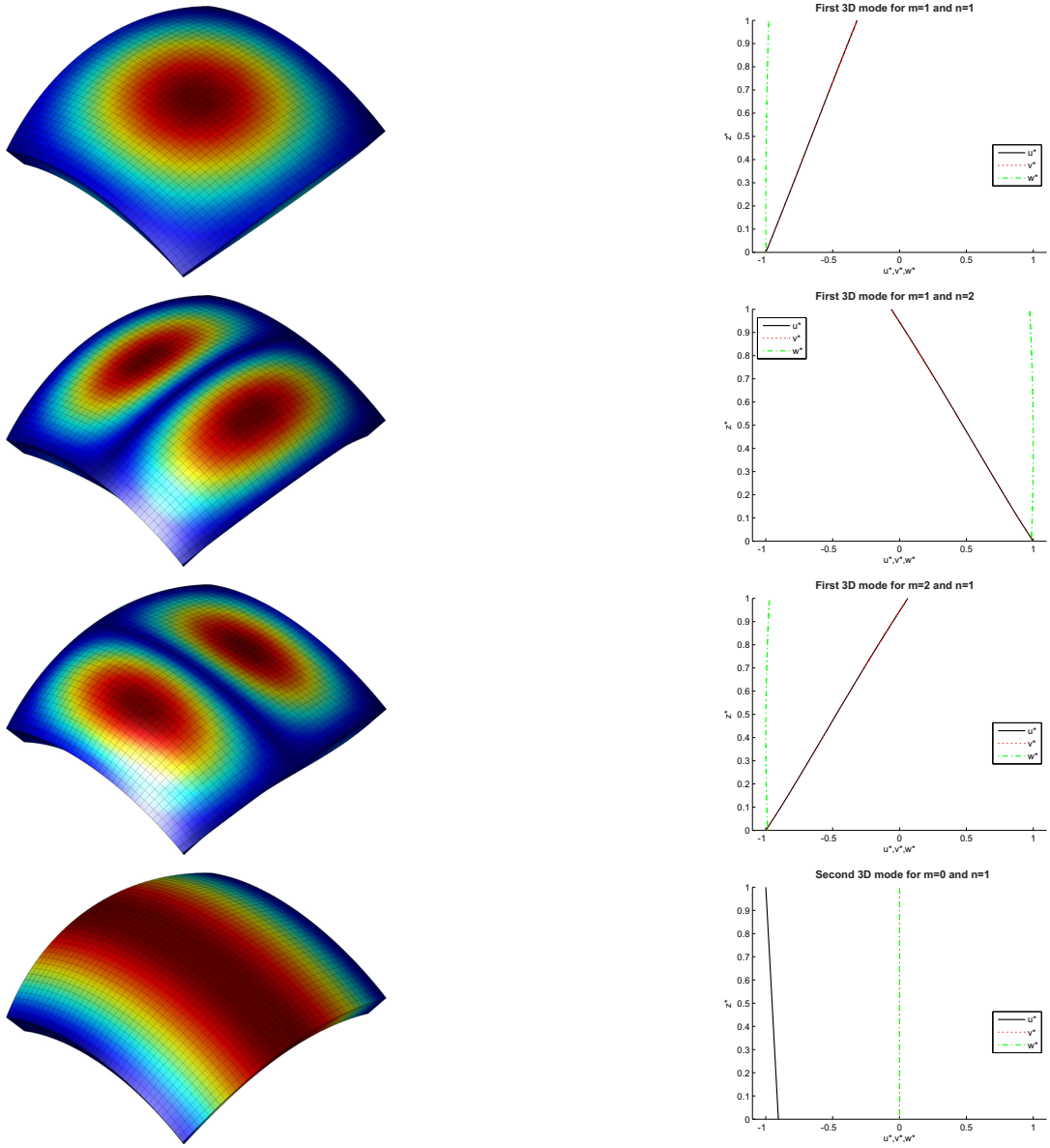


Figure 8: Simply supported sandwich spherical shell embedding FGM ($p$=1.0) core with thickness ratio $R_\alpha/h$=10. First four frequencies via 2D GDQ solution (on the left) and via 3D exact solution (on the right).